

**University of Alberta**

Thermogravimetric Analysis of Solvent Interaction with Model TSRU  
Tailings Components

by

Nesma Ansari

A thesis submitted to the Faculty of Graduate Studies and Research  
in partial fulfillment of the requirements for the degree of

Master of Science

in

Chemical Engineering

Department of Chemical and Materials Engineering

©Nesma Ansari

Spring 2013

Edmonton, Alberta

Permission is hereby granted to the University of Alberta Libraries to reproduce single copies of this thesis and to lend or sell such copies for private, scholarly or scientific research purposes only. Where the thesis is converted to, or otherwise made available in digital form, the University of Alberta will advise potential users of the thesis of these terms.

The author reserves all other publication and other rights in association with the copyright in the thesis and, except as herein before provided, neither the thesis nor any substantial portion thereof may be printed or otherwise reproduced in any material form whatsoever without the author's prior written permission.

*This thesis is dedicated*

*to*

*my parents*

## Abstract

Solvents are ubiquitously used in oil sands extraction industry to enhance the separation of bitumen froth. With developing new technologies such as non-aqueous bitumen extraction, the need to track solvent interactions with oil sands components throughout the extraction process and to identify potential causes of solvent loss is becoming increasingly important. While the use of solvents offers substantial processing gains, the loss of solvents to waste streams is not only expensive but also poses environmental concerns. Tailings solvent recovery units (TSRU) are used to recover solvent from the froth treatment tailings stream. With less than 100% solvent recovered, further research is required to better understand the unrecovered solvent. In the current study, the interaction of solvent with model tailings components is studied using thermal gravimetric analysis (TGA). The studies on solvent interaction with clays, asphaltenes and mixed systems confirm that operating temperatures higher than 100 °C are required to recover all the solvent. While unassociated or surface-wet solvent is easily removed, a small fraction of the solvent (paraffinic - 60% *n*-pentane, 40% *i*-pentane by mass) can be considered to interact with clays and strongly interact with asphaltenes. Approximately ~10% of the solvent interacts with asphaltenes and less than ~1% with 'clean' clays.

## **Acknowledgements**

First and foremost, I would like to express my sincere appreciation to my thesis advisors, Dr. Zhenghe Xu and Dr. Qingxia Liu for their supervision, guidance and help during the course of my thesis research. I would also like to thank Dr. David Harbottle, Dr. Yadollah Maham, and Douglas McKay for their continuous involvement during the experimentation and analysis part of this research and for providing valuable technical input.

I would also like to thank the Department of Chemical and Materials Engineering at the University of Alberta for the support of this research. Also, to the NSERC Industrial Research Chair for financial support.

I wish to express my thanks to Mr. Jim Skwarok, Ms. Jie Ru, and Ms. Lisa Carreiro for their continuous assistance with lab and office support. Also thanks to all my friends and colleagues, for their help in different phases of this work.

Last, but not least, I am deeply indebted to my parents for their endless love and continuous motivation throughout the duration of my studies. Thank you both for giving me the strength to stand strong and for giving me the foundation to be who I am. This thesis would not have been possible without the unconditional support from both of you. Also thanks to my siblings, Nazia, Ajaz bhai, and Saad, for the nonstop encouragement to give my best. To Ayaanu, for always bringing a smile to my face. Finally, I am genuinely grateful to my fiancé, Faraz, for always being there for me. Thank you for being ever-so understanding and patient with me during my many, many times of crisis.

# Table of Contents

|  |    |
|--|----|
| 1. Introduction.....   | 1  |
| 1.1 Research Objectives.....   | 3  |
| 1.2 Thesis Outline.....  | 4  |
| 2. Literature Review.....  | 6  |
| 2.1 Bitumen Froth Treatment Process.....                               | 7  |
| 2.1.1 Naphtha-based froth treatment.....                               | 8  |
| 2.1.2 Paraffinic froth treatment.....                                  | 8  |
| 2.1.3 Tailings Solvent Recovery Unit.....                              | 9  |
| 2.2 Asphaltenes.....   | 10 |
| 2.2.1 Asphaltene rejection with aliphatic solvents.....                | 11 |
| 2.2.2 Asphaltene precipitation.....                                    | 14 |
| 2.2.3 Fractionation of asphaltenes.....                                | 15 |
| 2.2.4 Self-aggregation of asphaltenes.....                             | 18 |
| 2.3 Non-aqueous Bitumen Extraction.....                                | 19 |
| 2.3.1 Pyrolysis.....   | 20 |
| 2.3.2 Solvent extraction.....  | 20 |
| 2.3.3 Solvent deasphalting (SDA) technology.....                       | 22 |
| 2.4 Solvent Dilution of Bitumen Froth Emulsion.....                    | 23 |
| 2.5 Organic Matter Adsorbed on Oil Sands Solids.....                   | 24 |
| 2.5.1 Insoluble organic matter (IOM).....                              | 25 |
| 2.5.2 Separation of organic matter from oil sands.....                 | 26 |
| 2.5.3 Insoluble organic carbon content (IOCC) of oil sands solids..... | 27 |

|   |    |
|---|----|
| 2.5.4 Organic rich solids associated with bitumen .....       | 27 |
| 2.5.5 Effect of organic rich solids on bitumen recovery ..... | 27 |
| 2.5.6 Tailings sludge accumulation .....                      | 29 |
| 2.6 Solvent Loss to Tailings.....                             | 30 |
| 3. Materials and Methods.....                                 | 32 |
| 3.1 Materials .....   | 32 |
| 3.2 Experimental Flowchart.....                               | 33 |
| 3.3 Preparation of Asphaltenes .....                          | 35 |
| 3.4 Dry Kaolinite and Dry Illite Samples .....                | 36 |
| 3.5 Steam-Wetting of Clays .....                              | 36 |
| 3.6 Effect of Solvent on Asphaltenes and Clays.....           | 37 |
| 3.6.1 Free solvent on dry asphaltenes and clays .....         | 37 |
| 3.6.2 Potential interaction of solvent with asphaltenes.....  | 38 |
| 3.6.3 Potential interaction of solvent with clays .....       | 39 |
| 3.7 Addition of Water to Solbit.....                          | 39 |
| 3.8 Addition of Clays to Solbit .....                         | 40 |
| 3.9 Mature Fine Tailings (MFT) Solids .....                   | 41 |
| 3.10 Equipment.....   | 41 |
| 3.10.1 TGA .....  | 41 |
| 3.10.2 Fourier Transform Infrared Spectrometer (FTIR) .....   | 44 |
| 4. Association of Asphaltenes with C5 Solvent.....            | 46 |
| 4.1 Pentane-Precipitated Dry Asphaltenes (C5A) .....          | 47 |
| 4.2 Surface-Wet Asphaltenes.....                              | 49 |

|  |    |
|--|----|
| 4.3 Precipitated Solvent-wet (SW) Asphaltenes .....                        | 50 |
| 4.4 Factors Affecting Solvent Association with C5A.....                    | 53 |
| 4.4.1 Time of secondary stage washing after precipitation .....            | 53 |
| 4.4.2 Effect of settling procedure.....                                    | 55 |
| 4.5 TGA Studies at Isothermal Conditions .....                             | 59 |
| 4.6 Chapter Conclusions .....  | 62 |
| 5. Thermogravimetric Study of Association of Solvent with Clean Clays..... | 64 |
| 5.1 Free Solvent in Clean Clays.....                                       | 64 |
| 5.1.1 Kaolinite.....   | 64 |
| 5.1.2 Illite .....   | 69 |
| 5.2 Association of Paraffinic Solvent with Clays .....                     | 73 |
| 5.2.1 Dry kaolinite .....  | 73 |
| 5.2.2 Dry illite .....   | 75 |
| 5.2.3 Water-wet kaolinite.....   | 76 |
| 5.2.4 Water-wet illite .....   | 77 |
| 5.3 Chapter Conclusions .....  | 79 |
| 6. Mixed Systems of Asphaltenes, Clays, Water and C5 Solvent .....         | 80 |
| 6.1 Water in Solbit System .....   | 80 |
| 6.2 Clays in Solbit System.....  | 82 |
| 6.2.1 Effect of dry and WW kaolinite in solbit.....                        | 82 |
| 6.2.2 Effect of dry and WW illite in solbit .....                          | 83 |
| 6.3 MFT .....  | 85 |
| 6.4 Chapter Conclusions .....  | 86 |

|  |    |
|--|----|
| 7. Conclusions and Future Work .....             | 87 |
| 7.1 Conclusions.....                             | 87 |
| 7.2 Future Work .....                            | 89 |
| 8. References.....                               | 91 |
| Appendix A: Water droplets added to dry C5A..... | 97 |



## List of Figures

|  |    |
|--|----|
| Figure 1 – 1. Generalized scheme for oil sands processing [5] .....  | 3  |
| Figure 2 – 1. A schematic of a bitumen extraction process at Syncrude [1] .....  | 7  |
| Figure 2 – 2. Idealized molecular structure of asphaltenes [21] .....  | 11 |
| Figure 2 – 3. Asphaltene content in bitumen after treatment with aliphatic solvents<br>at 25°C [13].....   | 12 |
| Figure 2 – 4. Asphaltene content in bitumen after treatment with <i>n</i> -pentane as a<br>function of temperature at S/B = 1.4 [13].....  | 13 |
| Figure 2 – 5. Mass loss curve for bitumen, maltenes, and asphaltenes precipitated<br>by pentane [22] .....   | 14 |
| Figure 2 – 6. (a) Micrograph of bitumen emulsion diluted with <i>n</i> -heptane at S/B =<br>1.0 [13] (b) Micrograph of bitumen emulsion diluted with <i>n</i> -<br>heptane at S/B=2.0 [13] ..... | 24 |
| Figure 2 – 7. Schematic of fractionation of oil sands into ‘active’ and ‘inactive’<br>components [45].....   | 26 |
| Figure 2 – 8. Conceptualisation of interaction of organic rich solids with bitumen<br>[45].....  | 29 |
| Figure 3 – 1. Particle size distribution of (a) kaolin and (b) illite.....   | 32 |
| Figure 3 – 2. Experimental layout of this study.....   | 34 |
| Figure 3 – 3. Wetting procedure for clays .....  | 34 |
| Figure 3 – 4. Schematic of a TGA [50] .....  | 43 |
| Figure 3 – 5. Schematic of the FTIR [52].....  | 44 |

|   |    |
|---|----|
| Figure 4 – 1. TGA profile of dry asphaltenes (C5A) for two runs of the same sample .....  | 48 |
| Figure 4 – 2. FTIR spectra of dry C5A.....  | 49 |
| Figure 4 – 3. Effect of increasing temperature on the weight loss of unassociated solvent added to dry C5A .....                                  | 50 |
| Figure 4 – 4. Thermogravimetric analysis showing association of solvent with solvent-wet asphaltenes (SW C5A) .....                               | 51 |
| Figure 4 – 5. Comparison of solvent-wet and surface-wet C5A with TGA .....  | 52 |
| Figure 4 – 6. TGA profile of dry coke and SW coke.....  | 53 |
| Figure 4 – 7. Effect of solvent-washing on SW C5A on the weight loss with increasing temperature .....  | 54 |
| Figure 4 – 8. TGA analysis of dry C5A soaked in C5 for different periods of time .....  | 55 |
| Figure 4 – 9. Schematic of centrifuged SW C5A vs. settled SW C5A.....   | 56 |
| Figure 4 – 10. Effect of settling vs. centrifugation of SW C5A on the weight loss with increasing temperature.....                                | 57 |
| Figure 4 – 11. Derivative plots from TGA for (a) dry C5A, (b) surface-wet C5A, (c) centrifuged SW C5A, and (d) settled SW C5A.....                | 58 |
| Figure 4 – 12. TGA profile of SW C5A at isothermal conditions as a function of time .....   | 59 |
| Figure 4 – 13. Derivative weight plot vs. time of SW C5A when held at isothermal temperature for (a) 30°C, (b) 40°C, (c) 50°C, and (d) 70°C ..... | 60 |

|   |    |
|---|----|
| Figure 4 – 14. Total amount of weight loss when held isothermal at specific temperatures.....   | 61 |
| Figure 4 – 15. Summary TGA profiles of dry C5A, surface-wet C5A, centrifuged SW C5A and settled SW C5A .....                          | 63 |
| Figure 5 – 1. Structure of kaolinite [60] .....   | 65 |
| Figure 5 – 2. FTIR spectra of kaolinite.....  | 65 |
| Figure 5 – 3. Effect of “free” solvent on dry and WW kaolinite .....  | 68 |
| Figure 5 – 4. TGA profile of WW kaolinite and water with the temperature ramp of 5°C/min up to 150°C, then 10°C/min up to 200°C. .... | 69 |
| Figure 5 – 5. Structure of illite [61] .....  | 70 |
| Figure 5 – 6. FTIR spectra of illite .....  | 71 |
| Figure 5 – 7. Effect of free solvent on dry and WW illite .....   | 72 |
| Figure 5 – 8. Weight loss as a function of temperature when dry kaolinite is mixed with C5 solvent for 24 hrs.....                    | 74 |
| Figure 5 – 9. Effect of increasing temperature on the weight loss of dry illite when mixed with C5 solvent for 24 hrs.....            | 75 |
| Figure 5 – 10. Weight loss vs. temperature of WW kaolinite when mixed with C5 solvent for 24 hrs .....                                | 77 |
| Figure 5 – 11. Effect of increasing temperature on weight loss of WW illite when mixed with C5 solvent for 24 hrs.....                | 78 |
| Figure 6 – 1. TGA profile of three tests of WW-SWC5A compared to TGA profile of only water.....                                       | 81 |

|   |    |
|---|----|
| Figure 6 – 2. Effect of dry/WW kaolinite in SW C5A on the weight loss with increasing temperature ..... | 83 |
| Figure 6 – 3. Effect of dry/WW illite in SW C5A on the TGA profile .....                                | 84 |
| Figure 6 – 4. Weight loss with increasing temperature when MFT solids are mixed with C5 solvent .....   | 86 |
| Figure A –1. TGA profile of water drop added to dry C5A compared to the profile of dry C5A .....        | 97 |
| Figure A – 2. Normalized data from Figure A-1 at 100°C to remove water .....                            | 98 |

## **Nomenclature**

C5 Solvent with 60% *n*-pentane and 40% *i*-pentane

C5A Pentane-precipitated asphaltenes

FTIR Fourier Transform Infrared Spectroscopy

H/C Hydrogen-to-carbon ratio

MFT Mature fine tailings

S/B Solvent-to-Bitumen ratio

SW Solvent-wet

TGA Thermogravimetric analysis

TSRU Tailings Solvent Recovery Unit

W/O Water-in-oil

WW Water-wet

# 1. Introduction

Bitumen is a heavy oil of very high viscosity, high density, and a low hydrogen-to-carbon ratio in comparison with conventional crude oils. Bitumen is converted into synthetic crude oil (SCO) and fractionated in refineries to produce gasoline, heating oils and diesel fuels.

Bitumen is sourced from a complex rock matrix that is generally referred to as oil sands, also known as tar sands or bituminous sands depending upon geographical location. Alberta, Canada has three designated oil sands areas (OSA): Athabasca Wabiskaw-McMurray, Cold Lake Clearwater and Peace River Bluesky-Gething. These three OSA's occupy an area of about 140,000 km<sup>2</sup>, making Alberta's oil sand deposits the largest in the world [1].

The density of bitumen is approximately 1.01 g/cm<sup>3</sup>, similar to water with a viscosity of about 100 Pa.s at 25 °C [2; 3], but the viscosity can be much higher (1000 Pa.s) at lower temperatures. Of the recoverable bitumen, it is estimated that 15-20% (140 billion barrels) is readily accessible by surface mining techniques. However, for the remaining 80-85% (2.4 trillion barrels), outside of the mineable region, greater than 75m, recovery by in-situ techniques such as SAGD (steam assisted gravity drainage) is readily applied. The total bitumen reserve is approximately 170 billion barrels, with an annual production of ~ 477 million barrels [4]. Energy Resources Conservation Board (ERCB) estimates bitumen production to more than double by 2018.

In the 1920s, Karl Clark developed a hot water based extraction process, known as the Clark Hot Water Extraction process (CHWE) to recover bitumen from oil sands. A generic flow diagram of oil sands mining and upgrading of bitumen is shown in Figure 1 - 1.

There are six basic processing stages in the surface mining of oil sands [5]:

1. Mining
2. Utilities
3. Extraction plant
4. Froth Treatment
5. Water Management: Tailings ponds/thickener
6. Upgrading facilities

All these units are inter-connected and hence, a holistic understanding is required to attain optimum performance throughout the process.

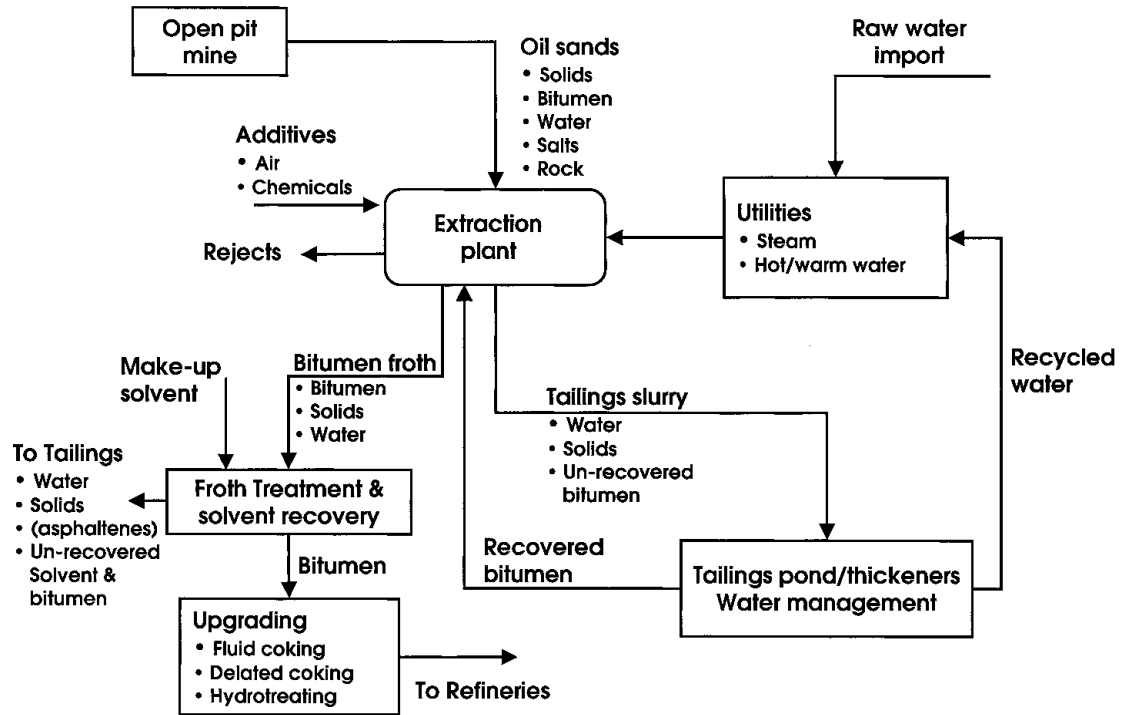


Figure 1 – 1. Generalized scheme for oil sands processing [5]

## 1.1 Research Objectives

A major challenge in froth treatment is the recovery of solvent that is added to assist in the separation of bitumen from water and fines. Unrecovered solvent will be lost with the tailings at both an economic and environmental expense. To comply with ERCB regulations, solvent losses should not exceed 4 bbl/1000 bbl of produced bitumen. The objective of this work is to develop a fundamental understanding of solvent interaction in froth treatment tailings to explain the difficulty of solvent recovery in the Tailings Solvent Recovery Unit (TSRU). Solvent interaction with precipitated asphaltenes, clean clays (kaolin and illite) were all assessed using thermogravimetric analysis (TGA). The critical condition for complete solvent removal is considered.



## 1.2 Thesis Outline

This thesis has been divided into seven chapters:

Chapter one: This chapter gives a general introduction and background to oil sands processing and the research objectives of the current study.

Chapter two: Provides a review on the most relevant literature considering froth treatment, asphaltenes, solvent interaction and extraction.

Chapter three: Describes the materials and methods that were used throughout the study. Equipment operational procedures are described in addition to sample preparation.

Chapter four: This chapter explains the interaction of solvent with asphaltenes and the different factors that affect such interaction. Surface-wet asphaltenes are differentiated from solvent-wet asphaltenes that have been centrifuged or settled. Solvent-wet asphaltenes under isothermal conditions are also investigated. The temperature at which the solvent is removed from the asphaltenes is presented.

Chapter five: This chapter explains the interaction of solvent with dry and wet clays such as kaolinite and illite. Free solvent on the clays is differentiated from solvent-wet clays. The temperature at which solvent-wet system is completely free of solvent is determined.

Chapter six: This chapter presents the interaction of solvent in a mixed system of asphaltenes, clays, and water. Solvent interaction with and without clays is

analyzed. In addition, solvent interactions with toluene washed MFT solids are studied.

Chapter seven: Overall project conclusions are presented along with suggestions for future research direction.

## 2. Literature Review

A typical bitumen extraction process employed by Syncrude Canada Ltd. is shown in Figure 2 – 1. The hot slurry from the hydrotransport pipeline is transported to a Primary Separation Vessel (PSV) where air is entrained to promote separation of the bitumen by allowing the bitumen to float to the surface. This bitumen froth is deaerated and then undergoes a froth treatment or cleanup process. The product from the froth treatment process is a relatively pure hydrocarbon (bitumen), sent to upgrading, where the hydrocarbon product is further processed to a synthetic crude oil [6]. The sulfur content of this synthetic crude is about 4.0 wt%. Conventional hydro-desulfurization processes are used to reduce the levels of both sulfur and nitrogen [7]. The middlings and tailings from the PSV are sent to the Tailings Oil Recovery (TOR) vessels, where the froth is recycled through the PSV again to improve quality. Bitumen recovered by the TOR vessels is processed by a secondary flotation plant and then combined with PSV primary froth.

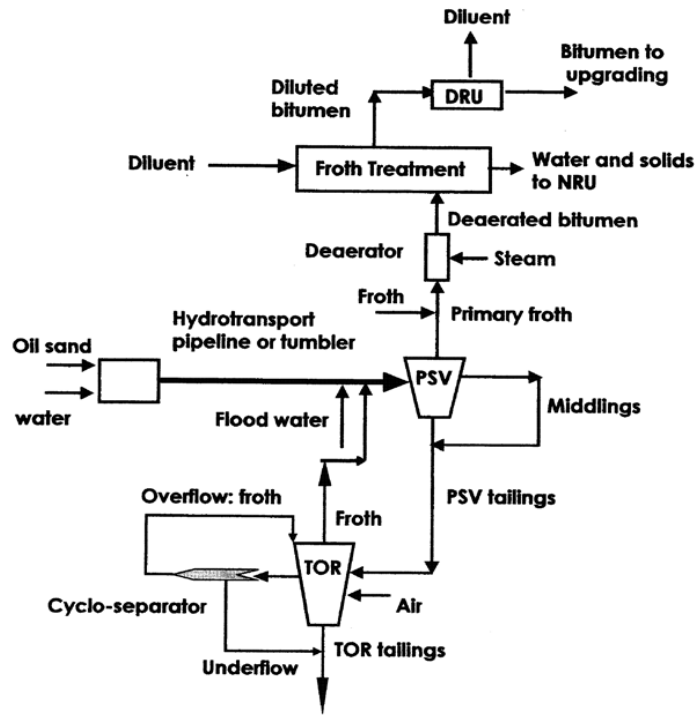


Figure 2 – 1. A schematic of a bitumen extraction process at Syncrude [1]

## 2.1 Bitumen Froth Treatment Process

Typically, bitumen froth is a highly viscous fluid that contains 60 wt % bitumen, 30 wt % water and 10 wt % solids [8; 9; 10]. With a high viscosity and the density almost matched fluids (water and bitumen), bitumen froth is diluted with a hydrocarbon solvent to enhance water – oil separation by inclined plate settlers, centrifuges, or hydrocyclones.

There are two types of froth treatment processes used in oil sands operations: naphtha-based and paraffinic treatments. Syncrude Canada Ltd., Suncor Energy and Canadian Natural Resources Ltd. utilize the naphtha-based process whereas

Shell Albian Sands use paraffinic treatment [11], mainly hexane as the solvent [12].

### **2.1.1 Naphtha-based froth treatment**

In naphtha-based froth treatment, bitumen froth is diluted with locally produced naphtha to remove water and solids. Operations currently use a naphtha to bitumen (N/B) ratio of 0.6 – 0.7 [13], below the critical ratio for the onset of asphaltene precipitation. Asphaltene precipitation was shown to occur at an N/B ratio of four and above [14].

To further clean the bitumen and remove any impurities, diluted bitumen (dilbit) undergoes multistage centrifugation (centrifugal force up to 2500 g) or separation via a series of inclined plate settlers [14]. The dilbit product consists typically of 2 – 5 wt % water and 0.5 – 1 wt % fine solids. The remaining water is less than 10  $\mu\text{m}$  in diameter and the residual solids are mostly dispersed clays [15]. Then, the dilbit is stripped off the naphtha in a Diluent Recovery Unit (DRU) while the froth treatment tailings are sent to the Naphtha Recovery Unit (NRU) to recover any leftover naphtha before the tailings are sent to the tailings ponds. The naphtha is recycled back to the froth treatment process and the dilbit product, now free of naphtha, is sent for upgrading.

### **2.1.2 Paraffinic froth treatment**

Paraffinic froth treatment uses paraffinic solvents such as pentanes, hexanes, heptanes or a combination of them. Recovered dilbit (also referred to as solbit) from solids and water is subsequently passed through the Solvent Recovery Unit

(SRU) to purify the product and recover solvent for recycle back into the froth treatment operation. The tailings from the froth settlers consist of water, solids (clays, silt, and coarse sand), heavy hydrocarbons (bitumen, asphaltenes) and entrained light hydrocarbon solvent. The tailings are then passed through the Tailings Solvent Recovery Unit (TSRU) to remove the majority of the paraffinic solvent by steam stripping [1], prior to ultimate disposal in the tailings ponds.

In paraffinic froth treatment, a diluted bitumen product consisting of less than 0.1 wt % water and solids is produced at a ratio higher than the critical solvent to bitumen (S/B) ratio [15]. This ratio corresponds to the onset of asphaltene precipitation, above which a very clean and dry bitumen product is produced [16]. The precipitated asphaltenes are rejected, with some released with the tailings stream.

Both froth treatment processes have their advantages and disadvantages. Paraffinic froth treatment gives a cleaner product but a lower bitumen yield compared with the naphtha-based froth treatment. Also there is a cost comparison with paraffinic solvents often more expensive; hence any solvent loss would also indicate an economic loss [17].

### **2.1.3 Tailings Solvent Recovery Unit**

The TSRU is a distillation unit that uses steam stripping to remove solvent from the tailings and recycle the solvent back into the froth treatment process. In the TSRU, light components (mostly hydrocarbon solvent) are separated from heavier

components (asphaltenes and minerals) under operating conditions of absolute pressure between 100 – 200 kPa and a temperature between 75 – 95 °C [18].

## 2.2 Asphaltenes

Asphaltenes are usually defined by a solubility class; a fraction insoluble in light alkanes such as *n*-pentane and *n*-heptane but soluble in aromatic solvents such as toluene [14; 19]. Asphaltenes consist of polyaromatic condensed rings with short aliphatic side chains containing heteroatoms such as nitrogen, oxygen, sulfur and various metals [20]. Asphaltene solubility is in part attributed to the interaction with resins. Changes in the asphaltene-resin balance due to pressure, temperature, and/or dilution (dilbit) can promote the onset of asphaltene precipitation [20]. The rejection of asphaltenes to tailings poses an environmental risk and an economic loss as potential usable hydrocarbons are discarded.

An idealized asphaltene molecular structure shown in Figure 2 – 2 was published by Groenzin and Mullins [21], where it was stated that on average, asphaltene molecules are composed of seven fused aromatic rings with diameters between 10 to 20 Å [21]. The average molecular weight of asphaltenes varies depending on the technique applied to measure MW, see later discussion in Section 2.2.3.

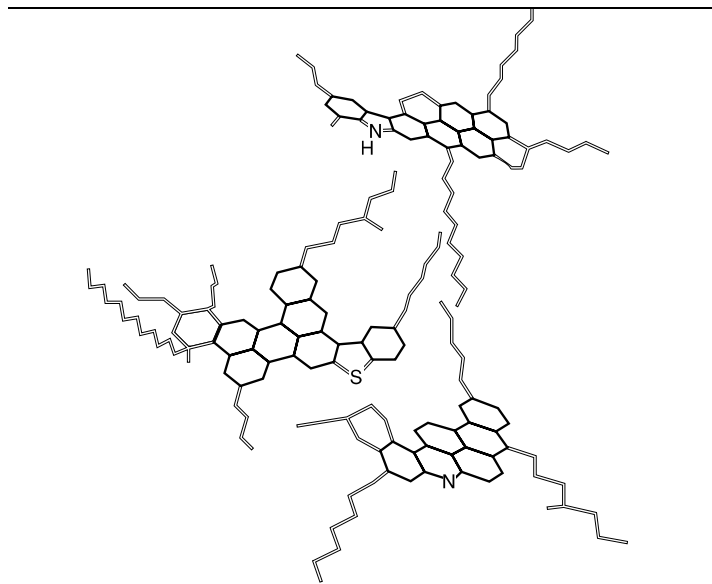


**Figure 2 – 2. Idealized molecular structure of asphaltenes [21]**

### **2.2.1 Asphaltene rejection with aliphatic solvents**

Asphaltene rejection from bitumen when treated with an aliphatic solvent depends on many factors including solvent type, solvent to bitumen (S/B) ratio, temperature and pressure [13].

Long et al. [13] treated bitumen with three solvents: *n*-pentane, *n*-hexane, and *n*-heptane at 25 °C. As shown in Figure 2 – 3, the lighter *n*-pentane rejects more asphaltenes than the heavier *n*-heptane at the same S/B; and asphaltene rejection increases with an increasing S/B ratio. At 25 °C, the critical S/B ratio for asphaltene precipitation is 1.0 for *n*-pentane, 1.35 for *n*-hexane and 1.6 for *n*-heptane [13]. Also, the aromatic content of the diluent influences the critical dilution, with the critical dilution ratio increasing with increasing aromaticity [14].



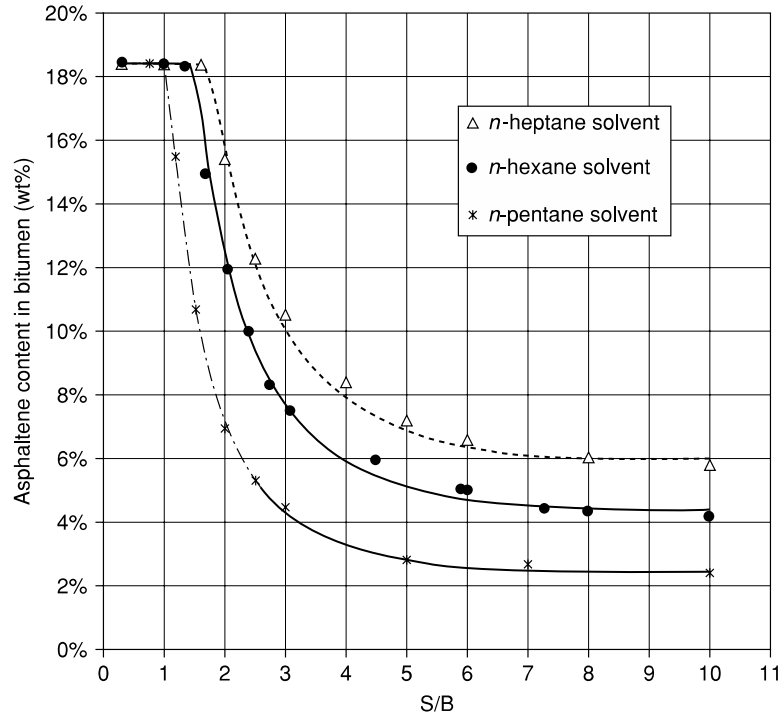


**Figure 2 – 3. Asphaltene content in bitumen after treatment with aliphatic solvents at 25 °C [13]**

Long et al. [13] also studied the effect of temperature on asphaltene precipitation after treatment of bitumen with *n*-pentane at S/B of 1.4 and 400 psi as shown in Figure 2 – 4. It was found that the solubility of asphaltene increases from 30 °C to 100 °C; however, as the temperature rises above 100 °C, the solubility decreases. It is hypothesized that the lower solubility of asphaltenes in *n*-pentane at higher temperatures may be due to an “excessive reduction in solvating power of the solvent” which causes reduction of its density at elevated temperatures [13].

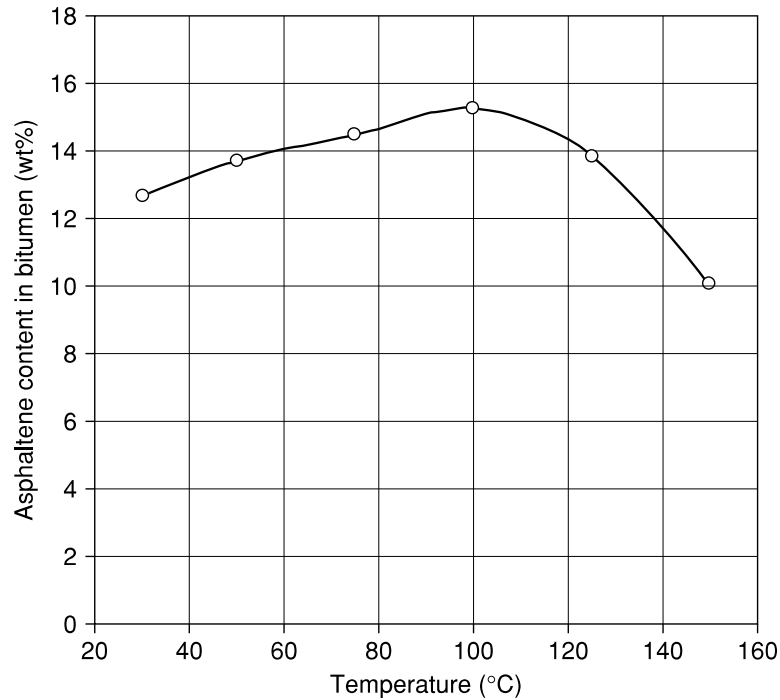


**Figure 2 – 4. Asphaltene content in bitumen after treatment with *n*-pentane as a function of temperature at S/B = 1.4 [13]**

Friesen et al. [22] carried out thermogravimetric analysis on asphaltenes precipitated from Athabasca bitumen using *n*-pentane as shown in Figure 2 – 5. Then, *n*-hexane at different S/B ratios varying from 1.1 to 3.5 was used to precipitate asphaltenes from the bitumen and heated up to a temperature of 1000 °C. TGA results showed that approximately 60 wt % of the asphaltenes decomposed at temperatures below 525 °C and that as the S/B ratio increased, the weight loss increased as well. Photoacoustic FTIR spectroscopy measurements also showed that as S/B ratio increased, the intensities of the hydrocarbon bands increased while those of the clay bands decreased [22].

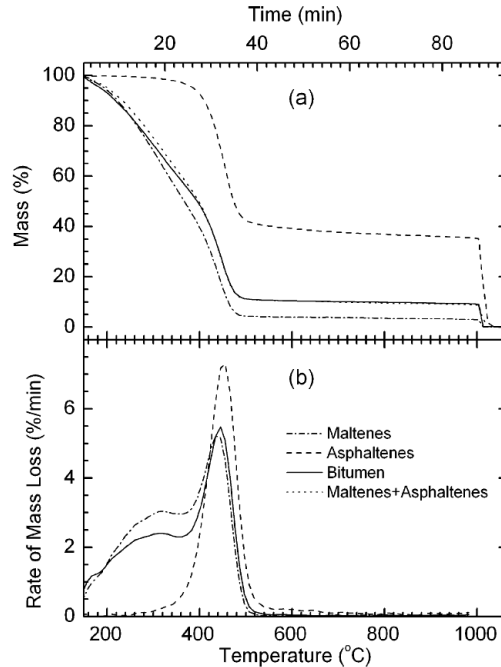


**Figure 2 – 5. Mass loss curve for bitumen, maltenes, and asphaltenes precipitated by pentane [22]**

### 2.2.2 Asphaltene precipitation

Athabasca oil sand bitumen contains about 17.5 wt % asphaltenes, 16.5 wt % saturates, 40 wt % aromatics and 26 wt % resins [2; 10], with an asphaltene rejection level of about 7 wt % for paraffinic solvents at their critical S/B ratio.

There are several methods for precipitation of asphaltenes. Yang et al. [3] precipitated whole asphaltenes from bitumen using *n*-heptane at a ratio of 40:1 S/B by volume and then recovered the precipitate through vacuum filtration. The asphaltenes were washed with *n*-heptane to remove any remaining maltenes and then mixed with toluene again and centrifuged to remove the remaining solids. Using a rotary evaporator, the supernatant was removed and the asphaltenes

collected and dried in a helium-flashed vacuum oven at 60 °C [3]. Friesen et al. prepared asphaltenes by using the ASTM method D3279-97 with *n*-pentane as the solvent [22]. Long et al. [10] used a mixture of CHCl<sub>3</sub> and *n*-pentane as the solvent to precipitate asphaltenes from Athabasca oil sands bitumen. The mixture was filtered and the precipitated asphaltenes washed several times with *n*-pentane until the filtrate was colorless. These asphaltenes were then dried at 50 °C [10].

### **2.2.3 Fractionation of asphaltenes**

Measuring the molar mass distribution of asphaltenes has been difficult because asphaltenes tend to self-associate to different degrees in different solvents. Different techniques such as elemental analysis, nuclear magnetic resonance (NMR), infrared spectroscopy (IR), vapor pressure osmometry (VPO), gel permeation chromatography and small angle neutron scattering have been used to understand the properties of asphaltene fractions.

Generally, asphaltene fractions are separated into subfractions from bitumen by adding a ratio of 40:1 of an alkane (either *n*-pentane or *n*-heptane) by volume [3].

Yarranton and Masliyah [23] fractionated a series of subfractions of Athabasca asphaltenes by using different heptane-to-toluene (H/T) ratios. The molar masses of these subfractions were determined from interfacial data and then compared with vapor pressure osmometry (VPO) values. It was found that as the toluene/hexane ratio increased, the asphaltene molecules had a higher molar mass as asphaltene precipitation decreased [23]. Yarranton and Masliyah [23] concluded that the solubility of asphaltenes in different solvents can be modeled

using a solid-liquid equilibrium calculation with K-values derived from Scatchard-Hildenbrand solubility theory which includes the Flory-Huggins theory.

Nalwaya et al. [19] fractionated asphaltenes using liquid/liquid extraction and studied the difference in polarities of different asphaltenes and analyzed the effects of metal ions, in particular  $\text{Fe}^{3+}$ , on asphaltene precipitation and dissolution [19]. Different fractions of asphaltenes were precipitated by mixing with a binary mixture of methylene chloride and *n*-pentane. As the amount of *n*-pentane increased, the polar effect of methylene chloride decreased; hence, the asphaltenes precipitated first were the most polar, followed by precipitation of less polar fractions upon the addition of more *n*-pentane. It was shown that asphaltenes precipitated in the presence of  $\text{Fe}^{3+}$  ions were significantly more polar than asphaltenes without  $\text{Fe}^{3+}$  [19].

Kaminski et al. [24] continued the work for classification of asphaltenes via fractionation, concluding that the more polar asphaltene fractions have smaller dissolution rate constants into DBSA/heptane or toluene solutions. For highly polar asphaltenes, dissolution is more difficult compared to the less polar fractions. Differential Scanning Calorimetry (DSC) showed that the more polar asphaltenes have a crystalline structure whereas the lower polar asphaltene fractions have an amorphous structure [20]. Later it was found that asphaltenes have a disc-like structure instead of a spherical structure as assumed previously [24].

Yang et al. [3] fractionated six subfractions of asphaltenes from Syncrude's coker feed bitumen by increasing the heptane-to-bitumen (H/B) ratio from 1.25 to 40. These subfractions were analyzed using elemental analysis, Fourier Transform Infrared Spectroscopy (FTIR) and VPO. Elemental analysis showed that lower carbon and hydrogen contents of precipitated asphaltenes from bitumen (P-1.25) compared to normal hydrocarbons. The fine solids were contaminated by a small amount of organic material, which could not be washed with toluene, similar to organic solids classified by Kotlyar [25]. FTIR showed that the lowest H/B ratio gave the highest aromaticity of the six subfractions and increasing ratio decreases aromaticity. VPO showed that asphaltene subfractions precipitated first have a lower molar mass than those precipitated later [3].

Yang and co-workers [3] concluded that water-in-oil (W/O) emulsion stabilities were highest in mixtures of asphaltene subfractions where the asphaltenes were partially soluble; however, lower W/O emulsion stabilities were seen with mixtures where asphaltenes were mostly soluble or mostly insoluble. Also, it was observed that as the H/B ratio increased, the hydrogen-to-carbon (H/C) ratio increased and the solubility in heptane/toluene mixtures increased. Solubility was more sensitive to the aromaticity of the solvent at lower H/B ratios compared to the sensitivity at higher H/B ratios [3].

#### 2.2.4 Self-aggregation of asphaltenes

Asphaltenes molecules tend to self-associate especially when thermodynamic equilibrium is disrupted. The first step in the precipitation of asphaltenes from oils is considered to be the self-association of asphaltene molecules [24].

The effect of solvents on the self-aggregation of asphaltene molecules was studied by Leon et al [26]. Critical nano-aggregation concentrations (CNAC) of asphaltenes were determined in cyclohexane, tetrahydrofuran, and carbon tetrachloride by surface tension analysis. The solubility parameter of asphaltenes with their CNAC values in different solvents was related through the Flory-Huggins interaction parameter [26]. This parameter is calculated in terms of the Hildebrand solubility parameter:

$$\chi = (\delta_a - \delta_s)^2 v_s / kT \quad (1)$$

where  $\delta_a$  and  $\delta_s$  are the asphaltene and solvent solubility parameters,  $v_s$  is the molar volume of solvent, and T is the temperature. Equations derived by van Krevelen were used to calculate the solubility parameter of the asphaltenes [26]. Leon et al. [26] concluded that asphaltenes with low hydrogen content and high aromaticity begin to aggregate at lower concentrations than asphaltenes with high hydrogen content and low aromaticity.

Mohamed and Ramos [27] studied pentane-insoluble (C5I) and heptane-insoluble (C7I) asphaltenes in pyridine, nitrobenzene and toluene by surface and interfacial tension measurements. They found that in both toluene and pyridine solutions, C5I showed a higher CNAC value, while C7I showed a higher CNAC value in

nitrobenzene solutions; this difference may be due to the possible formation of mixed aggregates [27].

Oh et al. [28] showed microscopic evidence for the aggregation of asphaltenes and measured the onset of asphaltene precipitation using near-infrared (NIR) spectroscopy. It was also concluded that as the solvent solubility parameters increased, asphaltene solubility increased.

When water-in-bitumen emulsions are treated with aliphatic solvents such as *n*-pentane, *n*-hexane, and *n*-heptane, emulsified water droplets, dispersed solids and precipitated asphaltenes form aggregates [29]. Long et al. [29] concluded that the effective aggregate density for the C5C6 solvent system was much higher than that for the C7 solvent. The authors also observed that by increasing the mixing temperature of the bitumen emulsion from 50 °C to 100 °C, larger aggregates formed thereby increasing the settling rate of the aggregates [29].

### **2.3 Non-aqueous Bitumen Extraction**

The CHWE process has been widely used to extract bitumen from the Athabasca oil sands for over 40 years. However, more recently non-aqueous bitumen extraction methods that are more robust are being considered as a substitute to the CHWE process. Two types of non-aqueous bitumen extraction include pyrolysis and solvent extraction.



### **2.3.1 Pyrolysis**

In the pyrolysis process, such as the AOSTRA Taciuk process, oil sand is heated through mixing with hot recycled sand [17]. A cyclone is used to separate the bitumen from its mineral solids after it has been cracked into light hydrocarbons and vaporized. Mineral solids contain small amounts of coke, which are burned to generate heat for the pyrolysis reaction [17]. However, because of the high temperatures required for heating, this method is not economically viable on a large scale. Also, this method is less desirable because of the high amounts of greenhouse gas emission released into the atmosphere.

### **2.3.2 Solvent extraction**

In the solvent extraction process, a solvent is mixed with the oil sands ore, lowering the viscosity of bitumen promoting favorable conditions for liberation and extraction. The recovered dilbit is then treated to separate out the bitumen, producing a clear solvent for recycle. Solvent loss to the tailings is minimized to reduce economic loss and environmental risk [7]. Apart from the robustness (good recoveries from poor ores) and GHG benefit, solvent extraction offers another advantage with minimal water consumption, and hence the reduction in tailings volume.

Meadus et al. [30] developed the first solvent extraction process for the Athabasca oil sands, which was a naphtha-based process. It was termed as Solvent Extraction Spherical Agglomeration (SESA) process. However, this process was unfeasible because of the large requirements of solvent for slurring of the oil sands feed.

Also, high solvent boiling point rendered solvent extraction expensive and difficult [30].

Funk et al. [31] developed a solvent extraction method using a low boiling point solvent to extract bitumen from tar sands. The solvent bitumen mixture passed through a classifier and then a countercurrent extraction column to recover the viscous bitumen and fines. Solvent was recovered from a two-stage fluidized-bed drying zone. The unbound solvent was removed and the sand water content was lower to less than about 2 wt % in the first fluid bed. The treated sand would then undergo a second fluid-bed drying zone fluidized by an inert gas, which was heated to a temperature to remove the bound solvent. It was predicted that this process will reduce the amount of solvent required to extract tar sands, minimize the energy requirements to recover solvent and maximize the amount of solvent recovered to at least 99 % [31].

Graham et al. [32] examined a solvent extraction method using *n*-heptane, separating the dilbit from the coarse sand using hydrocyclones and centrifuges and from the fines by *n*-pentane deasphalting. The solvent was then recovered by steam stripping the coarse tailings and by drying the fine tailings [32].

Wu and Dabros [17] investigated five different solvents at low solvent to bitumen ratios and their effect on bitumen recovery. Centrifugal and pressure filtration was used to separate the solvent and bitumen from the solids. The solvent in the filtration cake was recovered by vacuum evaporation at room temperature and then condensing the solvent vapor. Thermogravimetric analysis was used to

determine the residual bitumen content in the extracted mineral solids and the ash content in the bitumen product. It was found that cyclopentane and *n*-pentane were easier to recover than toluene [17]. Overall bitumen recovery of over 90 wt % was not achieved with centrifugal filtration. However, if a higher S/B ratio was used, regular pressure filtration results in a bitumen recovery of over 90 wt % [17]. Wu and Dabros [17] also concluded that for both high-grade and low-grade ores, bitumen recovery and bitumen quality from solvent extraction is comparable to bitumen recovery from the water-based extraction process.

Hooshiar et al. [33] used solvents at four different toluene-to-heptane (T/H) mass ratios to extract bitumen from both good processing and poor processing ores. It was observed that for the good processing ore, variation in the T/H ratio did not have an effect on the bitumen recovery; however, for the medium grade, poor processing ore, as the T/H ratio increased, bitumen recovery decreased [33].

### **2.3.3 Solvent deasphalting (SDA) technology**

Solvent deasphalting (SDA) technology utilizes a solvent to extract a deasphalted oil (DAO) stream from the bitumen feed, thereby separating them from asphaltenes. Deasphalted oil is also known as maltenes. KBR has developed processes that use solvents that are light hydrocarbons to extract DAO streams [34].

Earlier studies by Brons and Yu [35] showed bitumen recovery from the Cold Lake region of Alberta by using light hydrocarbon solvents such as *n*-pentane, *n*-butane, isobutane, and propane. The degree of deasphalting is highly dependent

on the length of the hydrocarbon solvent chain. Longer chains remove a smaller amount of asphaltenes because of a higher solubility of oil.

Four solvents (*n*-pentane, *n*-heptane, *n*-decane, and *n*-dodecane) investigated by Zou et al. [36] in the extraction of bitumen showed that dodecane gave the highest DAO yield and *n*-pentane gave the lowest DAO yield.

Al-Sabawi et al. [34] investigated SDA using the Athabasca bitumen feed and observed that a higher DAO yield leads to a smaller amount of asphaltene precipitation. Also, they concluded that a mixture of *n*-pentane/acetone results in the highest DAO yield when compared to conventional *n*-alkane solvents [34].

## **2.4 Solvent Dilution of Bitumen Froth Emulsion**

Bitumen froth emulsion stability is largely dependent on the type and nature of the solvent used. The solvent creates demulsification of water-in-bitumen emulsions by increasing the density difference between the oil and water phases and by lowering the viscosity of the oil phase.

As described by Tipman et al. [37], a paraffinic solvent was added to the bitumen froth to break the water-in-oil emulsion. The water was separated from the bitumen phase under gravity settling or centrifugation and a dry, clean bitumen product was produced. A series of settling tests with bitumen froth and *n*-heptane/toluene solvents with  $S/B = 0.7$  at 80°C were performed. Although asphaltenes have a greater solubility in aromatic solvents compared to aliphatic solvents, it was observed that water-in-bitumen emulsions could not be

completely demulsified by changing solvent aromaticity [37]. However, they could be treated at S/B ratios higher than the critical ratio. Using *n*-heptane as the solvent, an S/B ratio greater than 1.6, precipitation of asphaltenes was observed, see Figure 2 – 6.

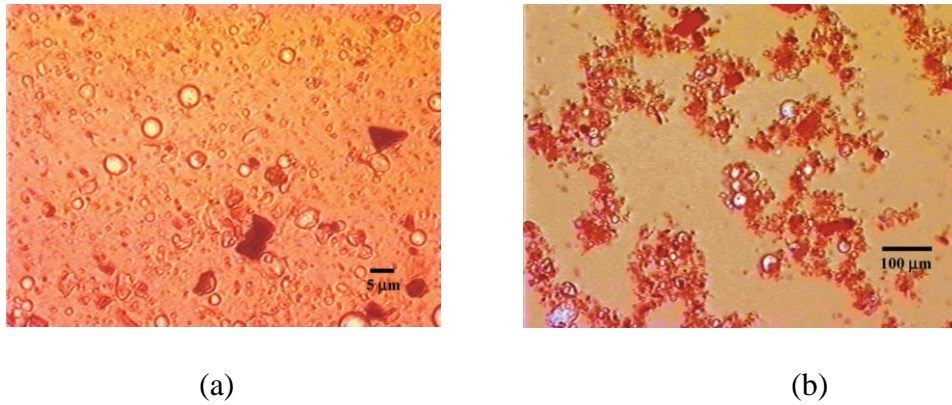


**Figure 2 – 6. (a) Micrograph of bitumen emulsion diluted with *n*-heptane at S/B = 1.0 [13] (b) Micrograph of bitumen emulsion diluted with *n*-heptane at S/B=2.0 [13]**

The dilution of bitumen froth with a paraffinic solvent (such as *n*-hexane) higher than the critical value of the S/B ratio as studied by Long et al. [15] shows that the resulting mixture forms large clusters of solids, water and precipitated asphaltenes which settle very easily, with no separation at S/B = 0.7.

## 2.5 Organic Matter Adsorbed on Oil Sands Solids

Canadian oil sands can contain a large percentage of fine solids which are to some extent contaminated by bituminous, organic matters [38]. Increased bitumen recovery tends to be associated with reduced fines and easier separation of bitumen from insoluble organic matter (IOM). The presence of this tightly bound organic matter was found in both oil sands ore and sludge [25; 38; 39; 40; 41; 42].

Two fractions of organic rich solids are defined:

1. Solids closely associated with bitumen
2. Solids isolated in an aqueous suspension

### **2.5.1 Insoluble organic matter (IOM)**

Organic matter, mainly composed of humic matter, cannot be removed by the bitumen extraction process as it is insoluble in solvents such as toluene. Most of the insoluble organic matter is strongly associated with fine solids (<45 µm) [43]. Kotlyar et al. [38; 39; 40; 44; 45] have carried out extensive research on organic rich solids, their association with bitumen and subsequent effect on bitumen recovery.

Organic rich solids can be classified into four categories:

1. Ultra-fine clays
2. Fossils
3. Heavy minerals
4. Aggregates

The organic rich solids have a tendency to stabilize emulsions and can also stabilize sludge structure [38].

Kessick [41] found that functional groups such as carbonyl, hydroxyl, and polyphenolic groups were present in organic matter closely associated with clays in oil sands and that organic matter “may consist of lignins in various stages of degradation” .

### 2.5.2 Separation of organic matter from oil sands

Organic rich solids can be separated from the oil sands ore using a Cold Water Agitation Test (CWAT), agitating with  $\text{Na}_2\text{P}_2\text{O}_7$ , centrifuging and separating into “active” and “inactive” components [40; 45]. Organic rich solids (ORS) are composed of biwettable, ultra-fine clays (ORS-BUF) and mineral aggregates (ORS-BAGG). These aggregates can be biwettable or completely hydrophobic, depending on their organic content. Hydrophilic, ultra-fines (HUF) are not composed of any organic rich solids. “Active” components of the oil sands ore are found to be more associated with toluene insoluble organic material (TIOM) [45].

The treatment scheme used for the separation is detailed in Figure 2 – 7 below:

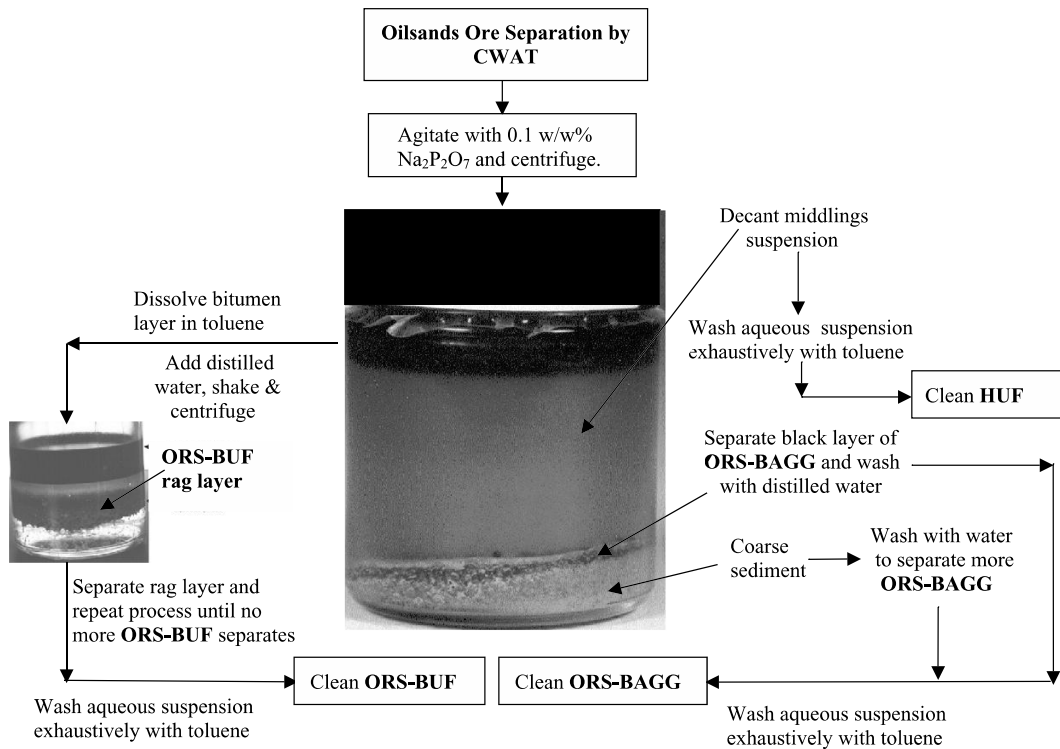


**Figure 2 – 7. Schematic of fractionation of oil sands into ‘active’ and ‘inactive’ components [45]**

### **2.5.3 Insoluble organic carbon content (IOCC) of oil sands solids**

Three fractions of oil sand solids using the CWAT procedure were separated from different grades of oil sands based on their various insoluble organic carbon content [40]. Bitumen solids (solids separated from the bitumen layer) had the highest insoluble organic carbon content (IOCC), followed by solids isolated from the aqueous suspension layer, followed by the remaining residual solids having the lowest IOCC. Elemental analysis showed that the organic rich solids were strongly associated with bitumen enriched in Fe, Ti, and Zr [40].

### **2.5.4 Organic rich solids associated with bitumen**

Kotlyar et al. [40] carried out a detailed study on the ORS strongly associated with bitumen by using a density separation method to separate the “organic rich solids into ‘free’ organic matter and organic matter mixed with inorganic matter”. Four fractions were obtained for each bitumen solids (BS) for the three oil sand grades (density varied from 1.6 g/cm<sup>3</sup> to 2.6 g/cm<sup>3</sup>) that consisted of different IOCC content. Elemental analysis on the four fractions showed that as the density of the BS fraction increased, the C, H, and N concentration decreased. However, the nature of the four fractions was similar as shown by the <sup>13</sup>C NMR spectra. It was also shown that aromatic carbon was the predominant type of carbon for all the samples.

### **2.5.5 Effect of organic rich solids on bitumen recovery**

Since the amount of associated organic rich solids (ORS) is largely correlated with bitumen, recovery of bitumen is affected as shown in Figure 2 – 8. Bitumen



association with ORS-AGG varies depending on the attachment at the oil-water interface, which can be strong, moderate (ORS-BAGG) or complete immersion in organic-rich hydrophobic aggregates (ORS-HAGG).

If the association of the organic rich solids with the bitumen is strong, the density of the bitumen increases to greater than 1 and results in the bitumen droplet going into the tailings streams. This un-liberated bitumen relates to steps 4, 5, 6, and 7 in Figure 2 – 8. However, if the association of the ORS with the bitumen is weak, then the liberated bitumen droplet will float and be collected in the froth, like the droplet labeled 1 in Figure 2 – 8. Therefore, the amount of ORS-BAGG content in any ore is a better predictor of ore processibility than bitumen, fines, or clay contents [45]. Although the bitumen that reports to the tailings stream is very small, knowledge of the separation of bitumen helps to improve and increase overall bitumen recovery and quality.

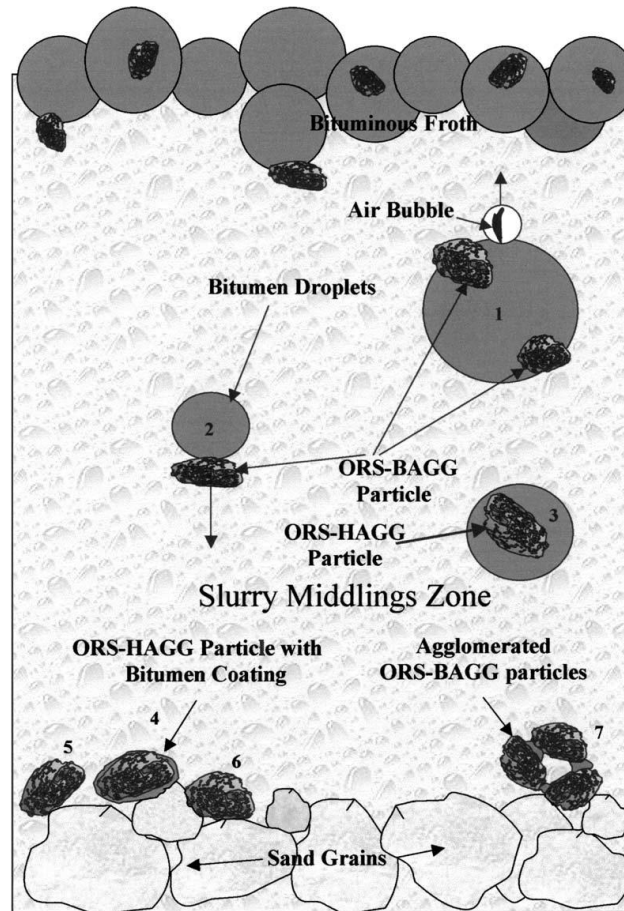


**Figure 2 – 8. Conceptualization of interaction of organic rich solids with bitumen [45]**

### **2.5.6 Tailings sludge accumulation**

The presence of unliberated bitumen, diluent and process water in sludge is a major issue promoting sludge accumulation in tailings ponds, providing an environmental risk. Oil sands fine tailings consist of a fraction of ultra-fine solids that are biwettable due to the presence of an organic coating on the particulate surfaces [25].

Using Soxhlet extraction to find out the composition of the tailings sludge, Kotlyar et al. [38] measured a composition of 71.2 wt % water, 28.0 wt % solids and 0.8 wt % bitumen. The tailings sludge (TS) was treated to extract asphaltenes and maltenes and to enrich solids with insoluble organic matter (TS). It was found that the TS layer contained the highest amount of insoluble organic carbon (14.9 wt %) compared to other layers such as the aqueous suspension of dispersed solids (AS) and residual solids (RS) [38].

## **2.6 Solvent Loss to Tailings**

Solvent losses should not exceed 4 bbl/1000 bbl of produced bitumen to comply with ERCB regulations. It would be ideal if an even lower target was achieved to avoid any environmental liability associated with solvent in the tailings area and to reduce solvent costs.

Naphtha evaporation from the oil sands tailings ponds was recently investigated by Kasperski et al. [46] from Canmet Energy. Recoverable bitumen was defined as the hydrocarbon that is not associated with mineral matter whereas unrecoverable bitumen was shown to have a strong affinity for hydrocarbons under the microscope. Thermogravimetric analysis was carried on the tailings after the tailings were centrifuged to separate the solids from the aqueous phase. Weight loss was measured and the composition of the evolved gases monitored using GC-MS to distinguish between water and carbon dioxide. Kasperski et al. [46] concluded that 40 % of the naphtha in the tailings is available to the environment and contributes to the volatile organic compounds (VOC's). It has

also been shown that if enough time is allowed for the diluent to be vaporized, it can be completely vaporized even at a lower temperature [46].

Afara et al. [47] from Canmet Energy investigated the interaction between the solvent, bitumen and mineral components in froth treatment tails and to quantify the volatile organic carbon or solvent escaping from the froth treatment tailings. Naphtha was added to samples containing bitumen, clay and MFT. A GC-MS/Flame Ionization Detection (FID) was used to analyze the gases being released by the sample. It was found that naphtha interacts more strongly with bitumen than with kaolinite and clay minerals from oil sands. Bitumen addition of 1.5 % released more than 20 % of naphtha. However, the addition of more bitumen did not change the levels of naphtha released. It was concluded that reducing the bitumen loss in froth treatment can help reduce solvent evaporation to the atmosphere [47].

### 3. Materials and Methods

#### 3.1 Materials

Coker feed bitumen provided by Syncrude Canada Ltd. was used, with asphaltene precipitating solvents *n*-pentane (ACS Certified) and 2-methylbutane (ACS Certified) [*i*-pentane] from Fisher Sci., Canada without further purification. Acid washed/USP kaolinite from Fisher Sci., Canada and illite from WARD's Natural Science, Canada were used as model clay particulates. The  $d_{50}$  of these clays was measured by using a Malvern Mastersizer 2000 particle size analyzer. Kaolinite  $d_{50} = 6.90 \mu\text{m}$  and illite  $d_{50} = 6.38\mu\text{m}$ . The particle size distribution for kaolinite and illite is shown in Figure 3 – 1. The precipitating solvent in all experiments was prepared using a mixture of *n*-pentane and *i*-pentane at a mass ratio of 60:40, respectively, equivalent to the paraffinic solvent used in industry.

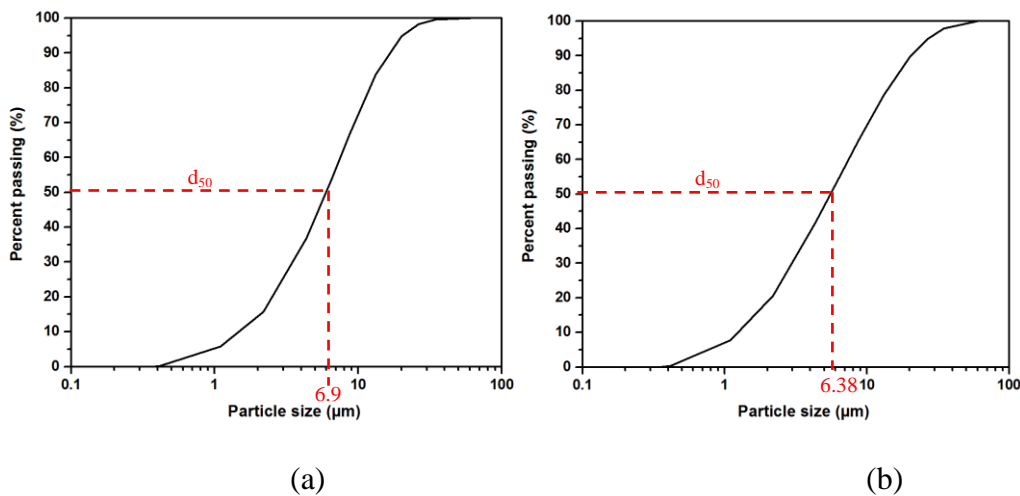


Figure 3 – 1. Particle size distribution of (a) kaolin and (b) illite

## 3.2 Experimental Flowchart

To better understand solvent interactions with model tailings components, a systematic series of experiments were considered. Figure 3 – 2 presents a layout of the experiments completed throughout the current study. Four key experimental areas (variables) for solvent interaction were considered:

- (1) Asphaltenes
- (2) Clays
- (3) Mixed Systems
- (4) MFT

The following abbreviations are used throughout the thesis:

WW: water-wet,

SW: solvent-wet,

C5A: pentane-precipitated asphaltenes.

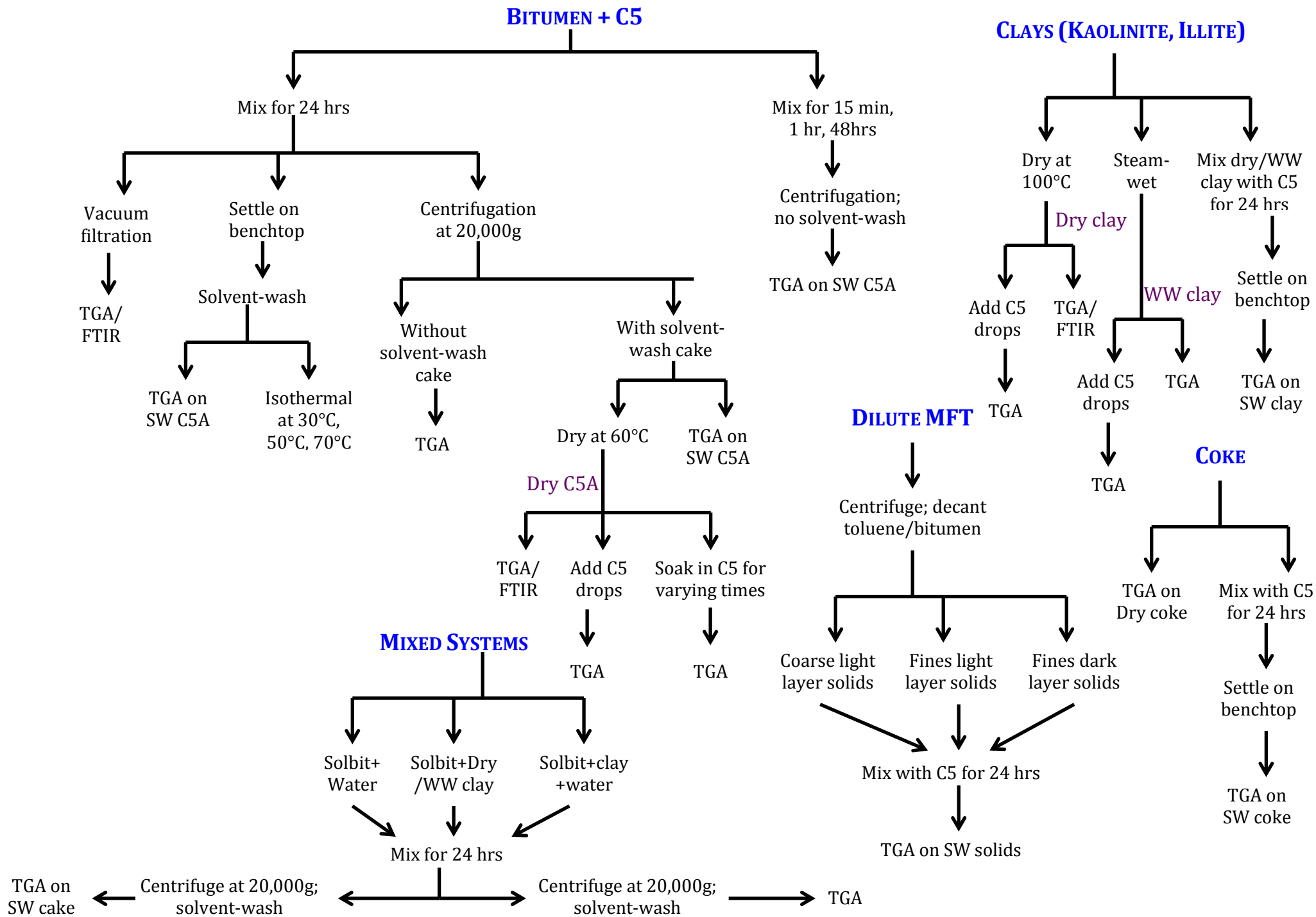


Figure 3 – 2. Experimental layout of this study

### 3.3 Preparation of Asphaltenes

Asphaltenes precipitated from bitumen separate into a light liquid phase (solvent-rich phase) and a heavy phase (asphaltene-rich phase). The particles that settle into a sediment layer are surrounded by an entrained continuous phase, which is the solvent-rich phase. The remainder of the continuous phase forms a layer of free solvent above the sediment. The solvent in the asphaltene-rich phase is of key interest in this study as this is the solvent that must be recovered for cost, safety and environmental reasons.

Asphaltenes were precipitated from coker feed bitumen using solvent (C5) above the critical dilution ratio. Diluted bitumen, referred to as solbit, was prepared by mixing bitumen and solvent at a mass ratio of 1:1.7 at room temperature. The solbit was shaken for 24 hours before centrifuging at 20,000 g for 30 mins at room temperature to deposit an asphaltene cake. The supernatant was removed and the wet cake re-dispersed in fresh solvent (60% *n*-pentane and 40% *i*-pentane) at a mass ratio of 1:1.7 cake:solvent and mixed for a further 15 mins in the shaker. Excess solvent was used to remove maltenes from the cake prior to analysis. Precipitated asphaltenes were then separated from the solvent via 15 mins of gravitational settling. One batch of asphaltenes was then dried in a vacuum oven at 60°C less than 10kPa for 48 hours to ensure all solvent was removed and the sample completely dried. The second batch was the SW asphaltenes used immediately for TGA measurements. These precipitated SW asphaltenes were



sealed in a vial and stored in a refrigerator by ensuring that the sample was kept solvent-wet at all times.

Another batch of asphaltenes was prepared by the same method as described above; however, instead of centrifugation, vacuum filtration was used to collect the asphaltenes. These asphaltenes were also washed with solvent again and dried in a vacuum oven at 60°C for 48 hours to ensure they are free of any solvent or water. Both batches of asphaltenes showed exactly the same results when analyzed using TGA.

### **3.4 Dry Kaolinite and Dry Illite Samples**

To remove any moisture from the clays, samples of about 10g of clay were dried in a vacuum oven at 100°C for 48 hours.

### **3.5 Steam-Wetting of Clays**

Two clay conditions were considered when interacting with solvent and asphaltenes: dry and water-wet. In the water-based extraction process, hydration of clays can prevent the adsorption of the hydrocarbon molecules on its surface. Therefore, the trapping of the solvent in clays with the presence of water is investigated.

The approach for hydrating the clays is depicted in Figure 3 – 3. 5 grams of either kaolinite or illite was placed in a filter paper cone, resting on a beaker filled with 20 mL of boiling water for 15 min. A glass lid was used to cover the top to ensure

no water vapor loss. In the procedure, water vapor penetrates through the filter paper contacting the solids, slowly hydrating and forming a thin water film around the clay particles.

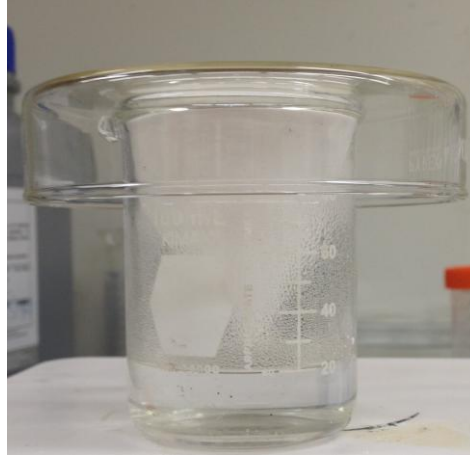


**Figure 3 – 3: Wetting procedure for clays**

### **3.6 Effect of Solvent on Asphaltenes and Clays**

To investigate different types of solvent interaction with either asphaltenes or clays, a series of controlled experiments were completed.

#### **3.6.1 Free solvent on dry asphaltenes and clays**

Initial experiments considered the rate of solvent weight loss from dry asphaltenes or clays immediately after solvent addition. With little solvent particle contact time, it was assumed that such an experiment would be very informative in terms of characterizing the removal rate of surface or ‘free’ solvent.

### 3.6.2 Potential interaction of solvent with asphaltenes

Following the precipitation procedure described in Section 3.2, SW asphaltenes were kept solvent-wet by ensuring a solvent layer remained above the deposited asphaltene cake in a sealed container and stored in a refrigerator. All batches analyzed were stored for less than 24 hours.

The interaction of solvent with asphaltenes (aggregated or dispersed) may also be dependent on factors such as:

- (1) **Time of secondary stage washing after precipitation:** To investigate if the washing step after asphaltene precipitation has any effect on the level of solvent interaction, a test was conducted to study the weight loss of SW C5A before and after solvent washing. In addition, another test was carried out to verify that the storage of asphaltenes in solvent does not affect interaction with the solvent. Dry asphaltenes were mixed in solvent for varying times (1 min, 5 min, 15 min, 2.5 hrs and 5 hrs) with solvent weight loss after washing measured using TGA.
- (2) **Effect of settling procedure:** Different settling protocols for the removal of precipitated asphaltenes after washing were considered to determine if the solvent interaction would be dependent on such procedure. The two protocols would most likely change the porosity of the asphaltene sediment and potentially influence the solvent interaction results. The first test precipitated asphaltenes by mixing the solbit for 24 hrs, centrifuging at 20,000 g for 30 min at room temperature, and then re-dispersing the wet cake in fresh solvent (60% *n*-pentane and 40% *i*-pentane) at a mass ratio

of 1:1.7 cake: solvent. These asphaltenes were mixed in a shaker for 15 min and separated from solvent by gravitational settling. The second test involved mixing the solbit for 24 hrs, followed by 15 min of gravitational settling, and finally re-dispersing the solvent-wet asphaltenes (after removing the supernatant) in excess solvent at a mass ratio of 1:1.7 C5A: solvent. These asphaltenes were also mixed for 15 min and separated via gravitational settling.

### **3.6.3 Potential interaction of solvent with clays**

To study the interaction of solvent with clays, clays were gently mixed for 24 hrs with solvent at a mass ratio of 1:34. This ratio is based on an assumption of 30 wt% clays in solids, which is typically composed of 60% bitumen, 30% water and 10% solids [38] and based on a 1.7:1 S/B mass ratio. Solids were separated from the solvent by settling for 15 mins. The solvent was then removed and the solvent-wet solids used for analysis. Both dry and wet clays (kaolinite, illite) were investigated.

### **3.7 Addition of Water to Solbit**

A mixture of water and solbit will form an emulsion with the water droplets stabilized by both soluble and insoluble asphaltene fractions. Experiments were conducted to consider the impact of water on solvent interaction with asphaltenes, with the results discussed in Section 6.1.

Tests were completed by mixing bitumen, solvent and water for 24 hrs at a mass ratio of 1:1.7:0.5, respectively. The ratio was calculated using a typical bitumen froth composition: 60 wt% bitumen, 30 wt% water and 10 wt% solids. The water and solbit mixture was centrifuged at 20,000g for 30 mins to collect the solids. The wet cake was re-dispersed in solvent at a mass ratio of 1:1.7 cake: solvent, mixed for 15 min in a shaker and left to settle for 15 min. These SW asphaltenes, which included trace amounts of water, were analyzed in the TGA quickly after removing the supernatant.

### **3.8 Addition of Clays to Solbit**

The solbit was prepared the same way as outlined in Section 3.1. 5 g of either kaolinite or illite were added to 50 mL of solbit solution. Four batches were prepared:

- (1) Dry kaolinite mixed with solbit for 24 hrs
- (2) Water-wet kaolinite mixed with solbit for 24 hrs
- (3) Dry illite mixed with solbit for 24 hrs
- (4) Water-wet illite mixed with solbit for 24 hrs

After mixing for 24 hrs, the clays were centrifuged at 20,000 g for 30 min. The supernatant was removed and the wet cake was re-dispersed in solvent at a mass ratio of 1:1.7 cake: solvent, mixed for 15 min in a shaker and left to settle for another 15 min. Washing the cake in excess solvent removed any maltenes that were present. The supernatant was removed again and the wet cake (solids and asphaltenes) was analyzed using TGA.

### **3.9 Mature Fine Tailings (MFT) Solids**

MFT solids were studied to understand the association of solvent with organic matter contaminated clays. These clays were studied because they are similar to the contaminated clays present in tailings. MFT was diluted with toluene at a volume ratio of 50:50 so that interactions of C5 solvent with toluene insoluble fractions, such as humic matter, could be studied. The diluted MFT was then centrifuged at 3000 rpm for 20 min. Three distinct layers separated after centrifugation: dark fines layer at the top, light fines layer in the middle and coarse solids at the bottom. These layers were removed and dried overnight at a temperature of 100°C. After drying, the solids were mixed for 24 hrs with the C5 solvent at a ratio of 1:34 to be consistent with the ratio used for mixing the “clean” clays with solvent. The mixture is left to settle with solids removed for immediate analysis with TGA.

### **3.10 Equipment**

#### **3.10.1 TGA**

Thermogravimetric analysis (TGA) is a highly sensitive (high precision) thermo balance in which weight changes correspond to environmental changes such as temperature in a controlled atmosphere. In the current setup, N<sub>2</sub> was used as the inert gas to remove the volatiles away from the sample. The pressure inside the TGA furnace was atmospheric pressure in our case, which is the case for the majority of TGAs.

The basic components of a thermobalance are [48]:

- (1) The Balance: null-point weighing mechanism where the sample remains in the same zone of the furnace irrespective of the change in mass [49]
- (2) The Sample Chamber: enables the work to be carried out in a controlled atmosphere at a controlled pressure. When the sample is heated, it is suspended from the balance beam and hangs down into the furnace
- (3) The Furnace: provides a uniform hot zone of sufficient length to completely contain the sample holder
- (4) Temperature Measurement: use of a thermocouple very close to the sample to measure temperature
- (5) The Temperature Programmer: provides a linear and reproducible set of heating rates and operates at a constant temperature with a stability of  $\pm 1$  °C or better
- (6) The Derivative Module: DTG trace can be simultaneously provided with the TG curve and can identify the point of maximum rate of weight change.
- (7) The Recording System: output is recorded in two ways: weight and temperature recorded as a function of time or weight is recorded directly as a function of temperature.

A schematic of the TGA is seen in Figure 3 – 4.

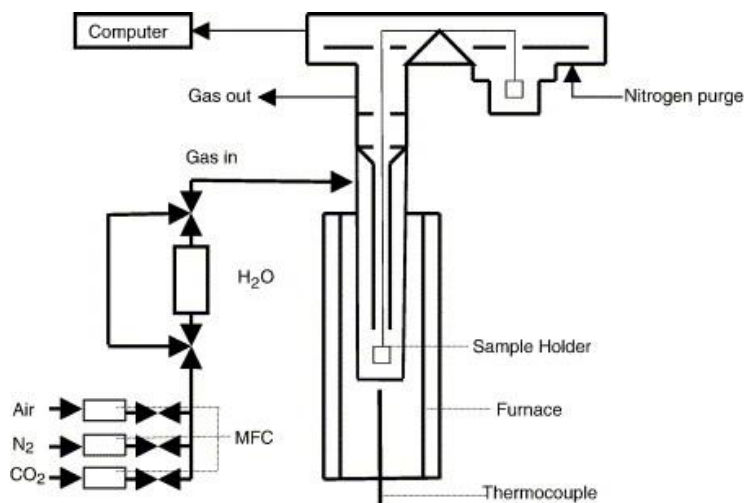


**Figure 3 – 4. Schematic of a TGA [50]**

Throughout the study, TGA Q500 (TA Instruments, Canada) was used. A solid sample of about 15-25mg was placed in a platinum pan holder. The thermocouple was aligned to ensure that it was as close to the sample pan as possible without physically touching the pan. The flow of nitrogen gas through the sample was kept constant at 80 mL/min. For all the experiments, a common heating procedure was implemented:

- (1) Heat the sample to 5°C/min until 150°C
- (2) Heat the sample at 10°C/min until 600°C.
- (3) Isothermal for 30 min at 600°C

Weight loss was measured as a function of increasing temperature to determine the level of solvent interaction. The main region of interest in this study was between 25°C and 150°C, the region where all solvent loss should be observed. Weight loss at temperatures greater than 150°C was most likely material decomposition.



### 3.10.2 Fourier Transform Infrared Spectrometer (FTIR)

Diffuse reflectance spectroscopy is widely used in FTIR analysis. This technique consists of a beam splitter, a fixed mirror, and a moving mirror. The beam splitter, splits the beam from the source into two; therefore, transmits only half of the radiation striking it and reflects the other half. One beam is transmitted to the fixed mirror, which passes to the detector, and the other half reflected back to the source. The radiation from the sample is converted into an electrical signal, which is then processed by the computer [51]. A schematic of the FTIR can be seen in Figure 3 – 5.

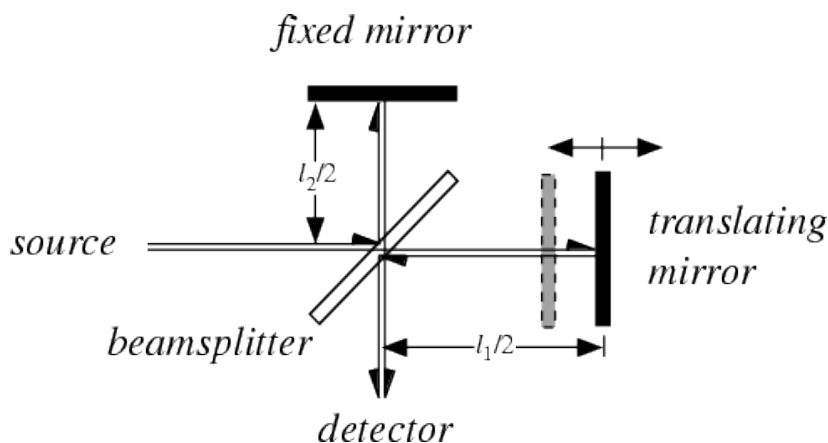


**Figure 3 – 5. Schematic of the FTIR [52]**

In our setup, BioRad FTS 6000 was used to obtain infrared spectra for dry C5A, kaolinite, and illite. This instrument can record infrared spectra in the range of  $400\text{ cm}^{-1}$  to  $11000\text{ cm}^{-1}$ . In order to use the FTIR, it was first important to cool the FTIR down with liquid nitrogen for 20 mins prior to any use. KBr was used as a reference sample and a background spectrum collected. Then, the sample was prepared by mixing 0.1g of KBr with ground 1-5 mg of sample and grinding the

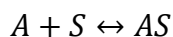
mixture in a mortar and pestle. This ground sample (now mixed with KBr) was placed into the sample holder and analyzed by diffuse reflectance. A Kubelka-Munk transform on the data was performed and the presence of bonds then analyzed.

## 4. Association of Asphaltenes with C5 Solvent

One possible source for solvent loss in Tailings Solvent Recovery Unit (TSRU) tailings could be due to the possible interaction of solvent with discarded asphaltenes.

Acevedo et al. [53] showed by Laser desorption ionization-time of flight mass spectrometry (LDI-TOF MS) that trapped solvent compounds present in asphaltenes result in “swelling”. Swelling in asphaltenes occurs by solvents due to the aliphatic chains connecting polycyclic units (PCU) [54]. A rosary-type structure for the asphaltenes was proposed by Acevedo et al. [53] that interconnects the PCU’s through the alkyl chain. These structures are very flexible and can take a large number of folded conformers. It has been said that in solvents such as toluene or similar solvents, this folded conformers prevail due to the aggregation tendency of the asphaltenes [54].

We know that in a typical quasi-irreversible process, the reaction between asphaltenes (A) and solvent (S) is given by:



It can be hypothesized that due to a high equilibrium constant, the reaction is favored and therefore displaces the equation to the right, thus encouraging the faster trapping of solvent within asphaltenes [53].

The focus of this chapter is to confirm if there is any interaction of solvent within asphaltenes studied by TGA. TGA signals of dry and solvent-wet (SW) asphaltenes will be compared. However, it is important to differentiate the possible interactions between the solvent and asphaltenes. Free or entrained solvent is solvent that is not interacting with asphaltenes, and is considered easily removed at room temperature. Solvent that strongly interacts with asphaltenes or considered to be “trapped” is removed at higher temperatures and identified as the problematic solvent. Furthermore, the factors that may influence solvent interaction with asphaltenes will be investigated.

In addition to the heat ramping tests, weight loss of SW C5A was also considered under isothermal conditions.

#### **4.1 Pentane-Precipitated Dry Asphaltenes (C5A)**

Asphaltene precipitated from bitumen and C5 solvent (which in this case is a mixture of 60% *n*-pentane and 40% *i*-pentane) after drying are analyzed with TGA. Figure 4 – 1 shows the effect of temperature on the weight loss from dry asphaltene for two tests, showing repeatability of TGA. Asphaltene decomposition starts around 400°C, where the majority of the weight loss is observed due to thermal degradation. In the temperature range of 25-150°C, there is no weight loss; hence, all solvent has been removed by the drying procedure. This TGA profile compares well with the TGA profiles of asphaltene shown previously [55]. These profiles form the control measurement from which solvent interaction can be studied.

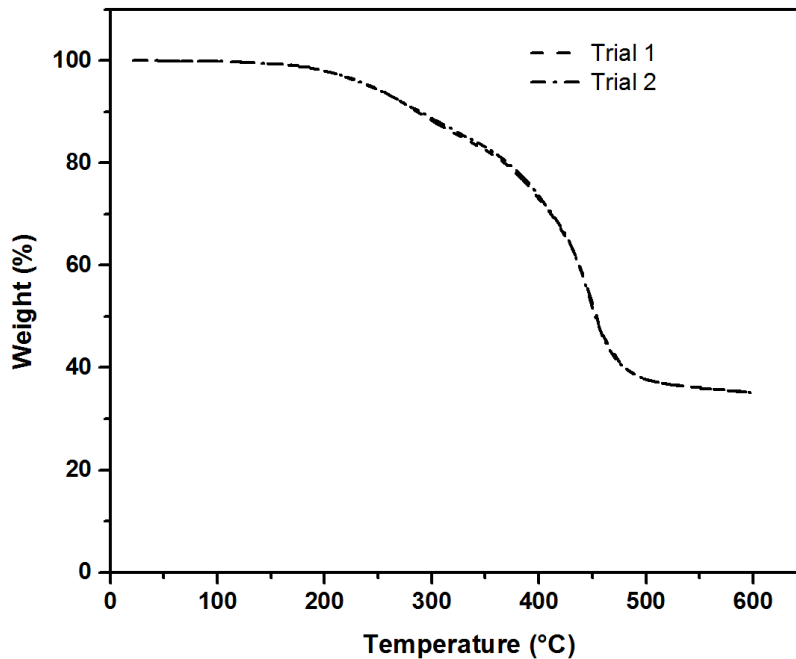


**Figure 4 – 1. TGA profile of dry asphaltenes (C5A) for two runs of the same sample**

The FTIR spectra of dry C5A can be seen in Figure 4 – 2. The typical peak for asphaltene is observed around  $2900\text{ cm}^{-1}$ , which shows the C-H stretching in both aliphatics and aromatics. The peak at  $3700\text{ cm}^{-1}$  shows the absorption bands for the OH group and the  $650\text{ cm}^{-1}$  to  $900\text{ cm}^{-1}$  represent the presence of aromatic rings [22].

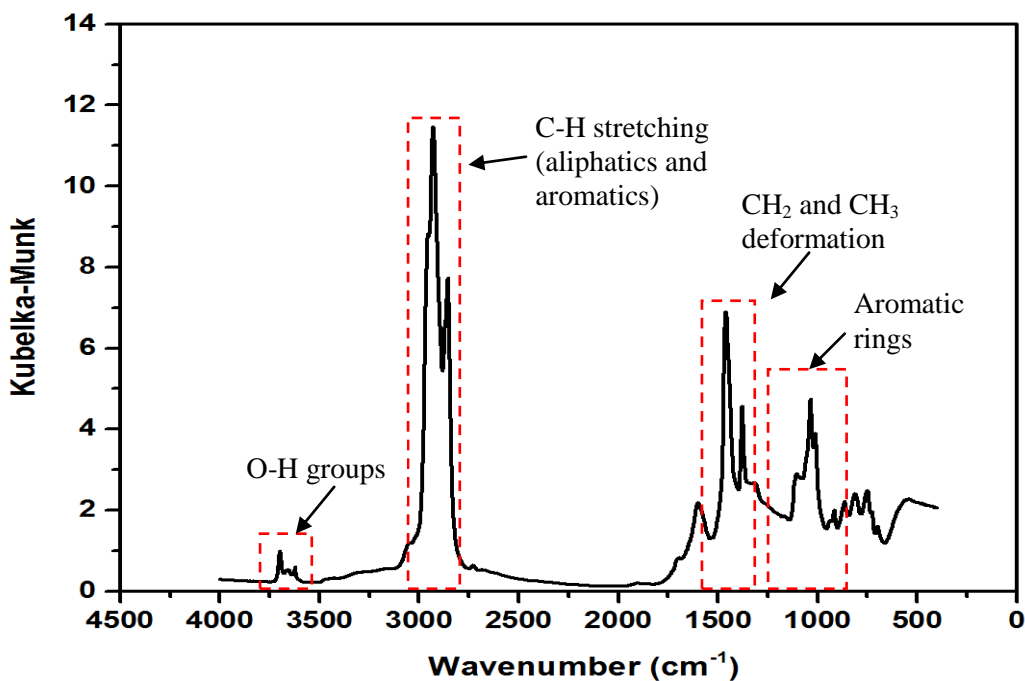
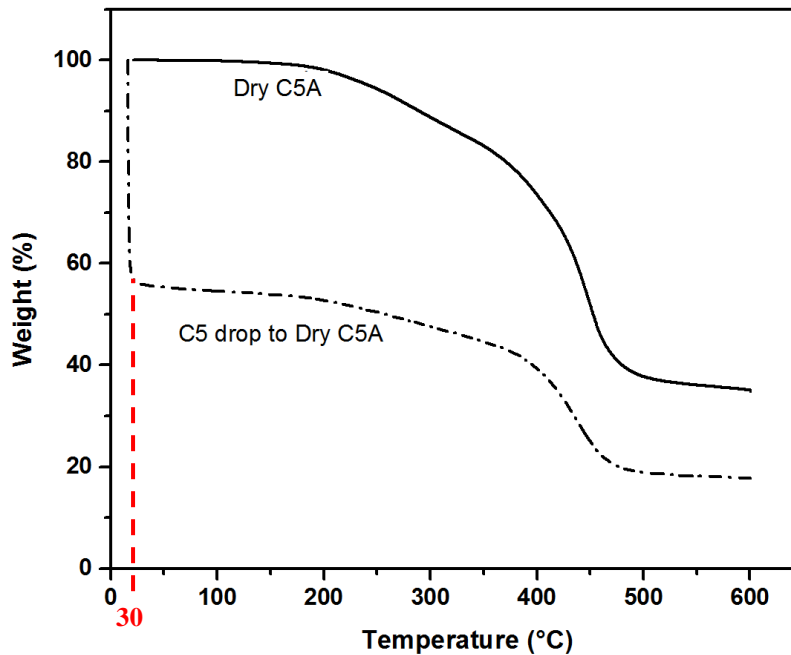


Figure 4 – 2. FTIR spectra of dry C5A

## 4.2 Surface - Wet Asphaltenes

Two to three drops of C5 solvent was added directly to dry asphaltenes in the TGA pan, with the test initiated immediately after addition. Figure 4 – 3 shows the TGA curve of free solvent on asphaltenes compared with dry asphaltenes. The droplets of solvent added to dry C5A shows rapid weight loss at low temperatures (< 50°C). Hence, the free or surface solvent is removed easily from the asphaltenes. In comparing the two drying rates, equivalent conditions are met at 30°C, which indicates that all added solvent has been removed. Such a test proves that solvent in contact with asphaltenes for a short time period is not difficult to remove, most likely indicating minimal solvent – asphaltene interaction.



**Figure 4 - 3. Effect of increasing temperature on the weight loss of unassociated solvent added to dry C5A**

### **4.3 Precipitated Solvent-wet (SW) Asphaltenes**

Solvent-wet (SW) asphaltenes (no drying after solvent wash) were also studied to investigate the possible solvent-asphaltene interaction. Asphaltenes samples were stored in a sealed container and kept solvent-wet at all times.

Two experiments with SW asphaltenes analyzed using TGA are shown in

Figure 4 - 4 and compared in Figure 4 - 5 with dry asphaltenes and free solvent on dry asphaltenes. A gradual decrease in weight loss (~ 24 %) measured up to ~110°C, indicates that the type of solvent interaction is distinctly different from the free solvent case in which all solvent was removed at temperatures below 30°C. In the current experiment, after 110°C, the drying rate (weight loss rate) for

SW C5A becomes equivalent to that of dry C5A. Such an experiment demonstrates that solvent interaction with asphaltene can be significant, and that the critical temperature for complete solvent removal is above 100°C. Such high temperatures for solvent removal are potentially due to the trapping of solvent inside asphaltene aggregates.

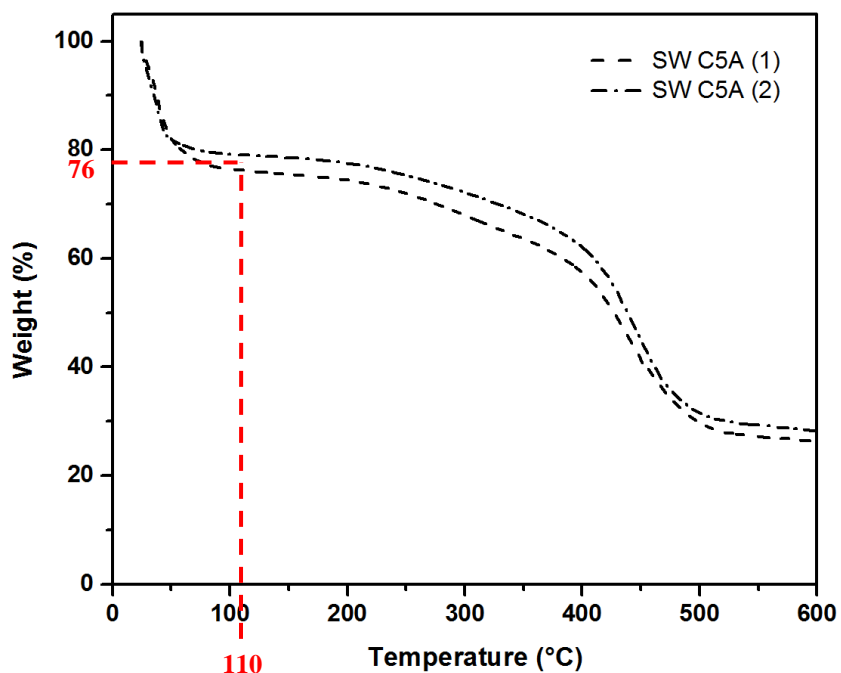


**Figure 4 – 4. Thermogravimetric analysis showing association of solvent with solvent-wet asphaltenes (SW C5A)**

Liao et al. conducted several simulations and found an abundance of micro porous structural units exist inside asphaltenes [56; 57]. Previously, there had been some observation of saturated hydrocarbons occluded inside the asphaltene aggregates. These occluded components are well protected by the asphaltenes and do not tend to be exchanged with the bulk phase [56; 57]. Also, in the presence of solvent,



the asphaltenes tend to form a flexible rosary-type structure that can easily trap molecules and isolate it from the environment [54].

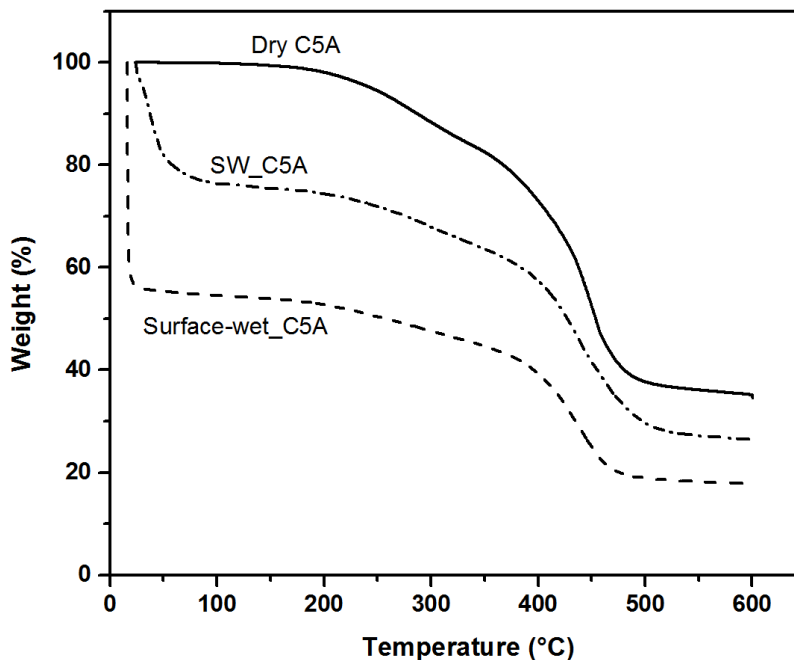


**Figure 4 – 5. Comparison of solvent-wet and surface-wet C5A with TGA**

In an attempt to better understand the nature of solvent interaction with asphaltenes, a test was conducted using fluidized coke. With a very low porosity, any possible interaction is expected to relate to the porous network between individual particles. Such a test is designed to better understand the interaction of solvent within a particle network.

A coke-solvent mixture was gently stirred for 24 hrs and then left to settle under gravity for 15 min. The SW coke was immediately transferred to the TGA for analysis. Figure 4 – 6 shows that there is no interaction of solvent with the coke,

and that any solvent retained in the porous network after sedimentation and removal is released at low temperatures (~ room temperature). Such behavior would confirm that solvent in particle network is not difficult to remove. This thinking can also be applied to the asphaltene case, which underlines that the mechanism for solvent – asphaltene interaction is much stronger (occlusion within the asphaltene aggregates).

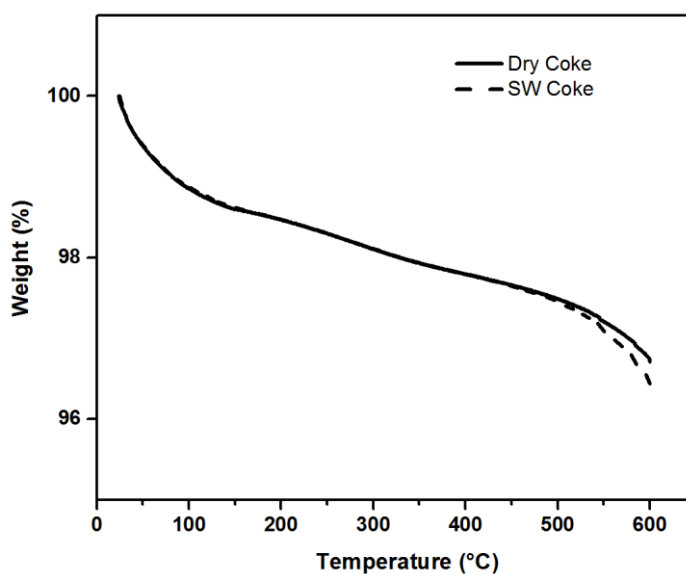


**Figure 4 – 6. TGA profile of dry coke and SW coke**

## **4.4 Factors Affecting Solvent Association with C5A**

### **4.4.1 Time of secondary stage washing after precipitation**

The washing of solvent-wet asphaltenes in excess solvent could potentially influence the degree of solvent interaction after precipitation. A SW sample washed in excess solvent for 15 minutes was compared with a SW sample not

washed (after 24 hrs of mixing the bitumen with C5 solvent, the precipitated asphaltenes are removed from the solbit and measured directly without excess solvent washing), as shown in Figure 4 – 7. The results indicate that washing increases slightly the solvent interaction with the asphaltene sample. The difference is approximately ~ 5 wt% but should not be considered within error. Repeat experiments were found to have an error less than 0.5 wt%.

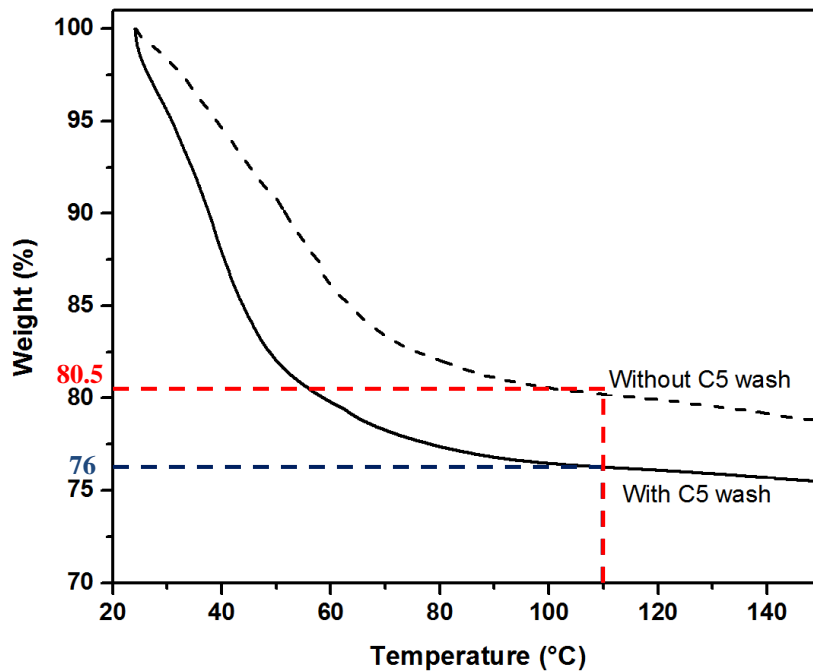


**Figure 4 – 7. Effect of solvent-washing on SW C5A on the weight loss with increasing temperature**

To better understand the impact of washing, dry C5A asphaltenes were washed in solvent for different periods of time (1 min, 5 min, 15 min, 2.5 hrs and 5 hrs). Figure 4 – 8 shows the solvent interactions (weight loss) with asphaltenes. It should be noted that in all cases, asphaltenes were separated by settling under

gravity. As shown in Figure 4 – 8, after 15 mins of mixing in solvent, the amount of solvent interaction appears to be independent of mixing time. The data also confirms that the washing step after precipitation may enhance the level of solvent interaction. Such observation would also support the earlier finding of solvent washing and solvent not washing (Figure 4 – 7). Soaking in solvent for 1 min also shows some degree of solvent - asphaltene interaction, ~ 5 wt% up to 100°C, indicating that the kinetics of interaction is relatively fast.

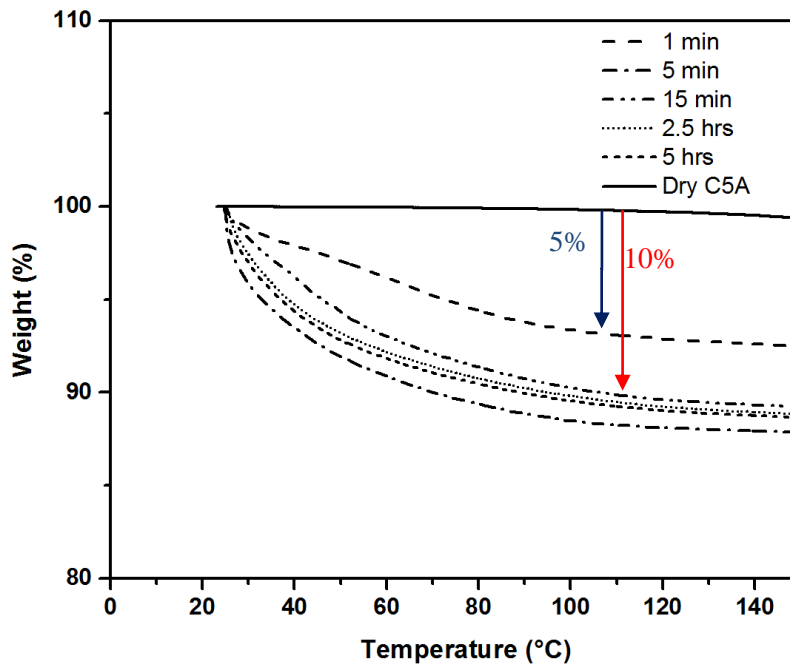


**Figure 4 – 8. TGA analysis of dry C5A soaked in C5 for different periods of time**

#### **4.4.2 Effect of settling procedure**

Another factor that may impact the amount of solvent interaction with asphaltenes is the settling procedure. By separating under gravity, the particle network pores

should be open, similar to the coke experiments. As such, network solvent is released at low temperatures. However, by centrifugation the particles are squeezed together forming a tightly packed network, which may restrict the removal of network solvent. Such a change in the structure may artificially indicate a higher level of solvent interaction due to restriction by the closing of network pores. It is important to identify if the settling protocol influences the apparent solvent interaction so that a correct conclusion on the amount of solvent interacting with asphaltenes can be formed.

A schematic to help explain the discussion is shown in Figure 4 – 9. Free solvent is easily removed when the SW C5A is settled under gravity compared to centrifuging where solvent is potentially “trapped” in tight network pores.

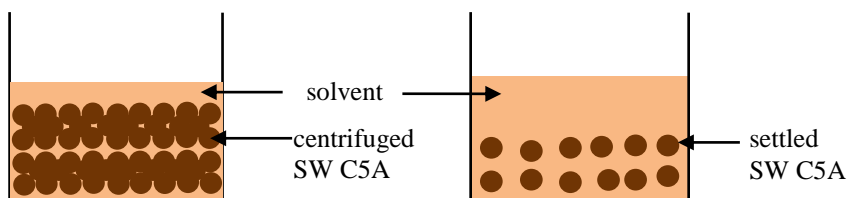


**Figure 4 – 9. Schematic of centrifuged SW C5A vs. settled SW C5A**

Figure 4 – 10 shows the TGA profiles for the settled SW C5A (no centrifugation) and centrifuged cases. Both samples are solvent-washed for 15 min for direct comparison and the thin layer of solvent removed to ensure a similar amount of asphaltenes. As shown, gravity settling of the asphaltenes produces a smaller weight loss as compared to the centrifuged sample. Gravity settled C5A indicate approximately 10 wt% solvent interaction up to 110°C, whereas centrifuged C5A

show a much higher weight loss, 24 wt%, up to 110°C. Above 110°C the rate change (% weight) for the settled SW C5A, centrifuged SW C5A and dry C5A becomes equivalent. The results confirm our previous discussion on the impact of centrifugation. Centrifugation of C5A not only accounts for true solvent interaction, but also solvent trapped within the tight network pores. Also, the settled SW C5A have more exposed free solvent that is easily evaporated before the sample is analyzed with the TGA. In all cases, a temperature above 110°C is sufficient to remove any solvent from the asphaltenes and its sediment.

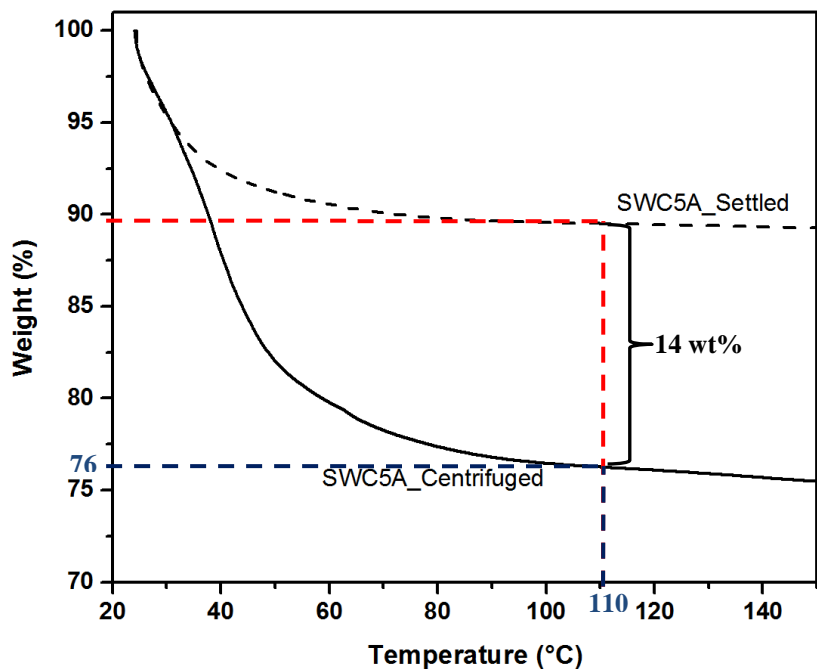


**Figure 4 – 10. Effect of settling vs. centrifugation of SW C5A on the weight loss with increasing temperature**

The derivative plots for dry C5A, surface-wet C5A, centrifuged SW C5A and settled SW C5A are shown in Figure 4 – 11. Dry C5A have a derivative weight loss of 0 until 150°C. Surface-wet asphaltenes start with a high weight loss rate, showing a sharp drop-off in weight loss rate to zero almost immediately.

Centrifuged SW C5A reaches a maximum rate and then the derivative weight loss goes to zero. The derivative weight loss for settled SW C5A drops off to zero at a more gradual rate. The rates are about zero (hence equivalent) at 110°C. At this temperature, the surface-wet C5A and the SW C5A have completely removed the solvent from the system, and now represent a dry C5A system.

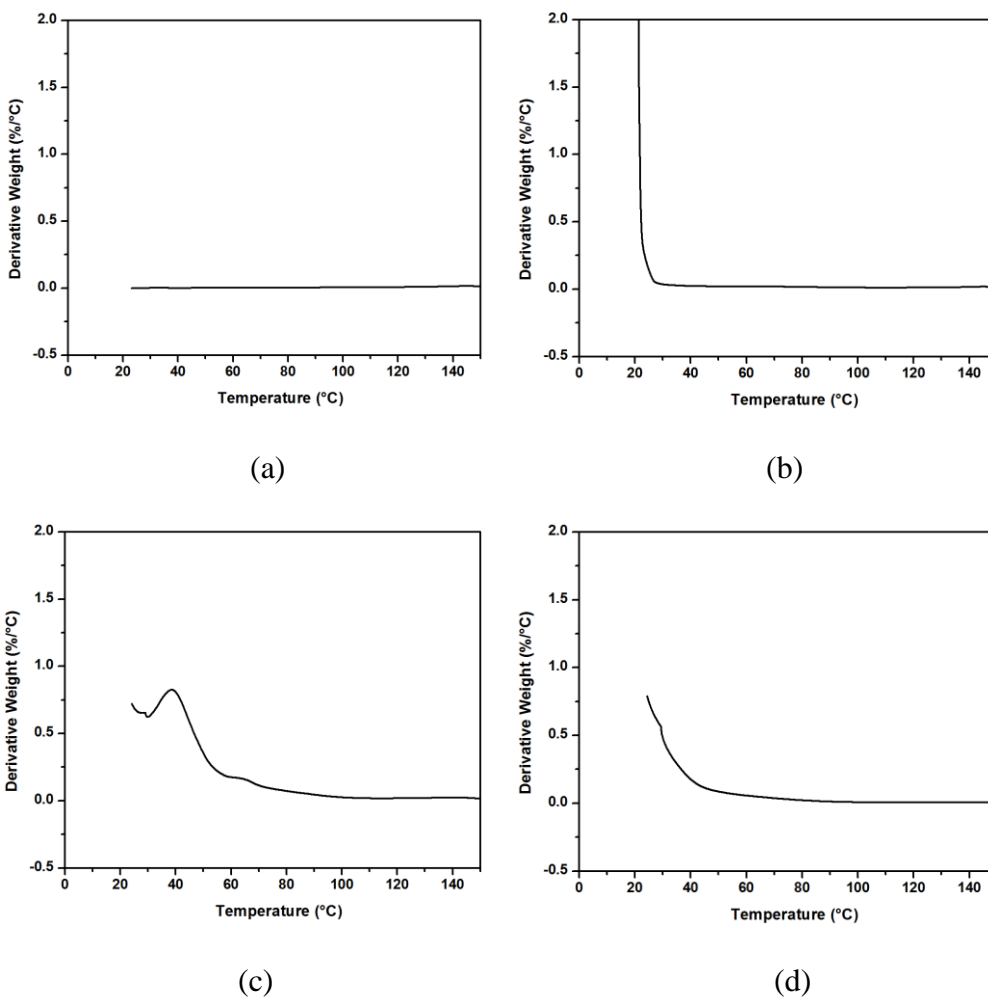


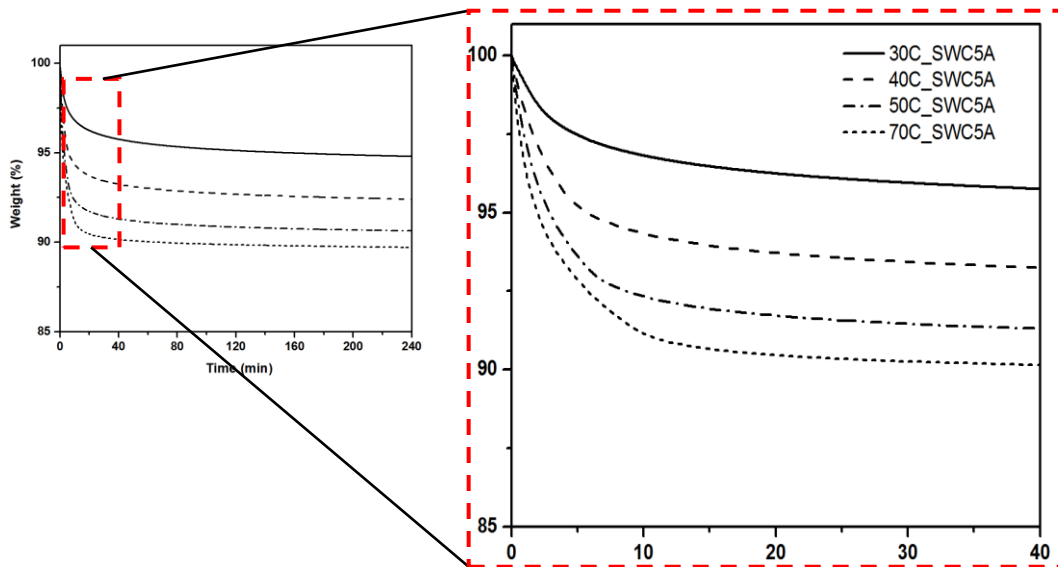
**Figure 4 - 11. Derivative plots from TGA for (a) dry C5A, (b) surface-wet C5A, (c) centrifuged SW C5A, and (d) settled SW C5A**

## 4.5 TGA Studies at Isothermal Conditions

SW C5A precipitated are settled under gravity for 15 min, washed in excess solvent (following standard protocol) and studied under isothermal conditions.

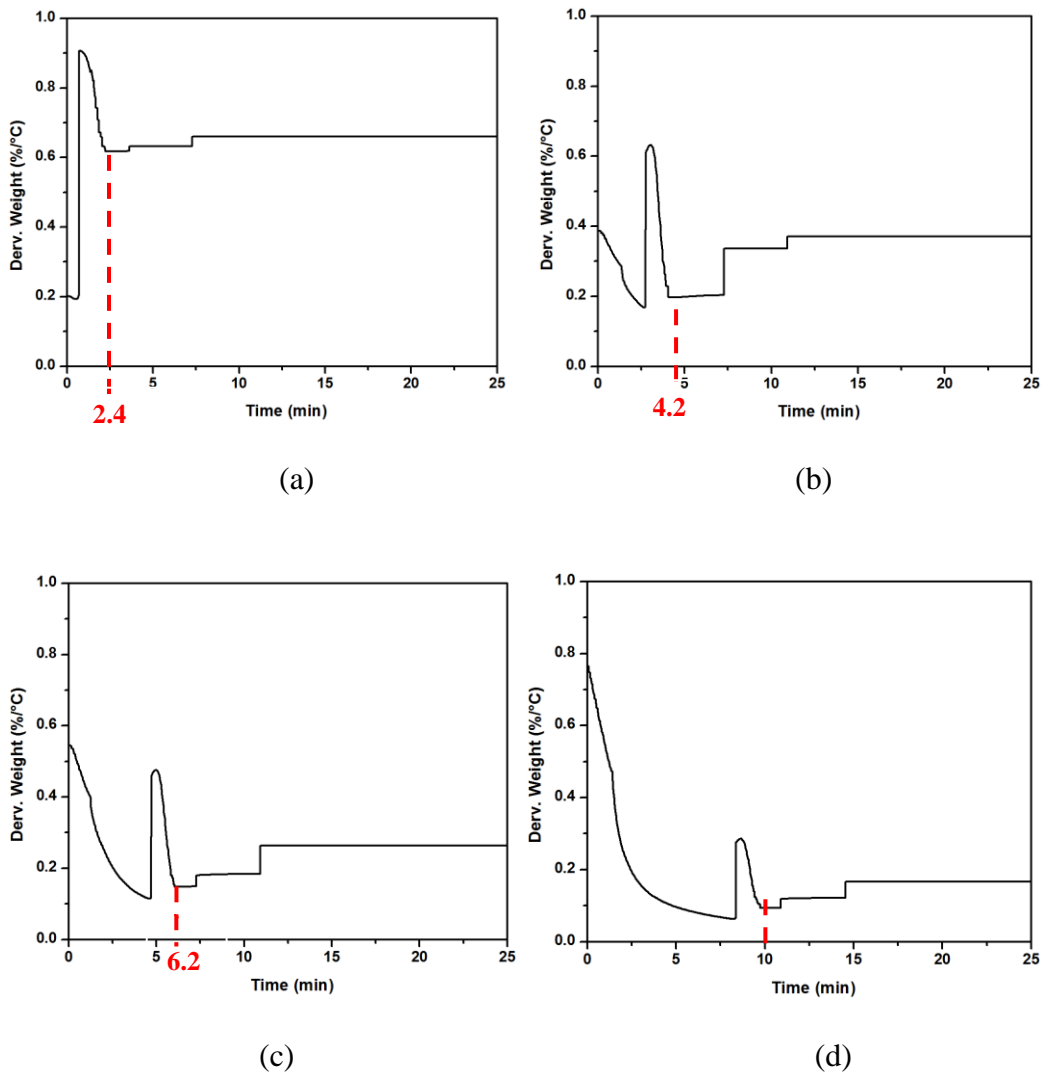
Four experiments were conducted where SW C5A were held for 4 hrs under isothermal conditions (30 °C, 40 °C, 50 °C, and 70 °C) before temperature ramping to 600 °C. TGA profiles for each test are shown in

Figure 4 – 12. As seen, after a specific time, weight loss reaches a plateau. As shown previously for dry C5A, the derivative weight loss is 0 until 150°C (see Figure 4 – 11). These systems do not remove any more solvent after a set period of time. The time to reach such condition increases as the isothermal temperature is increased. Hence, as temperature increases, more weight loss is observed, and a longer time is required to remove solvent from SW C5A, as seen in Figure 4 – 13.



**Figure 4 – 12. TGA profile of SW C5A at isothermal conditions as a function of time**





**Figure 4 – 13. Derivative weight plot vs. time of SW C5A when held at isothermal temperature for (a) 30 °C, (b) 40 °C, (c) 50 °C, and (d) 70 °C**

Figure 4 – 14 shows the amount of solvent released (based on total weight) at 30°C, 50°C, and 70 °C after 10 hrs. The total weight loss for each condition increases with increasing temperature. Yarranton et al. [58] performed drying

experiments with *n*-pentane precipitated asphaltenes, dried in a vacuum oven at 50°C in a stagnant nitrogen atmosphere until no change in weight was observed. It was shown that the solvent content with *n*-pentane is about  $3.5 \pm 1$  wt%. In the current study, keeping the temperature constant at 50°C, the total weight loss measured is around 9.6 wt%, greater than the weight loss observed by Yarranton et al. [58]. This higher weight loss is due to the flow of nitrogen over the sample which speeds up the evaporation process in our study versus a stagnant nitrogen atmosphere. However, the weight loss observed under isothermal conditions is comparable to the weight loss observed when the temperature was ramped up (see Figure 4 – 4). At 70°C, the weight loss observed for settled SW C5A is 10 wt%, which is comparable to the 10.5 wt% observed under isothermal conditions.

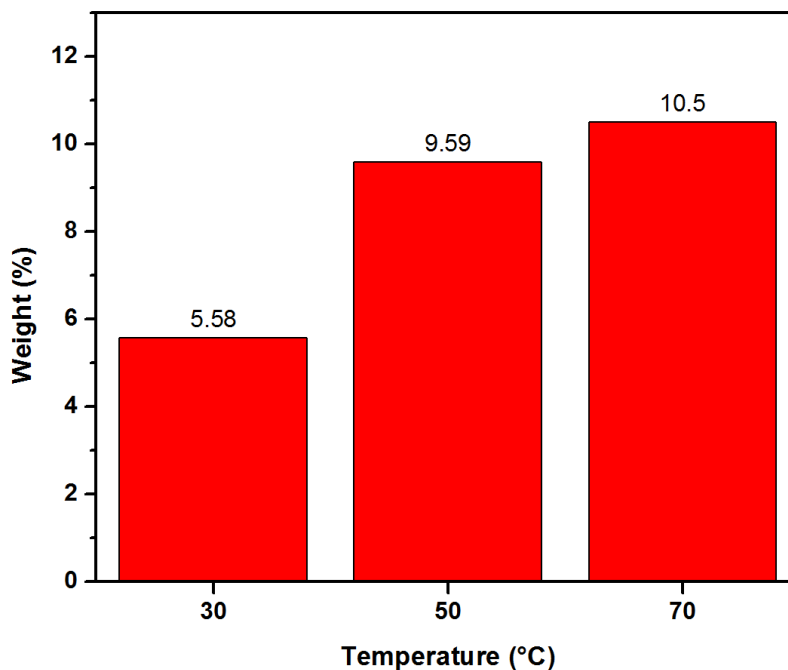


**Figure 4 – 14. Total amount of weight loss when held isothermal at specific temperatures**

## 4.6 Chapter Conclusions

In this chapter, the interaction of solvent with asphaltenes was studied. The various types of solvent interaction (surface-wet or trapping of solvent by centrifugation or settling) were analyzed with the TGA as seen in Figure 4 – 15.

Dry asphaltenes lose no weight until 400 °C, where they start to decompose. Free solvent on dry asphaltenes will tend to surface-wet the asphaltenes and shows minimal interaction. These surface-wet asphaltenes remove the solvent completely at 30°C.

Solvent-wet asphaltenes, on the other hand, associate more with the solvent. SW C5A that have been centrifuged account for true solvent interaction and solvent trapped within the tight network pores, hence showing about 24 wt% solvent. Settled SW C5A, on the other hand, have more open particle network pores, similar to coke, and allow for the solvent to be released at lower temperatures, hence showing an interaction of only 10 wt%. In both cases, at a temperature of 110°C, this solvent is completely removed from the SW C5A and the asphaltenes resemble a dry system. This may be one reason why the solvent in TSRU is not completely recovered because the column is operating at a lower temperature than the temperature required to completely remove the solvent from the asphaltenes.

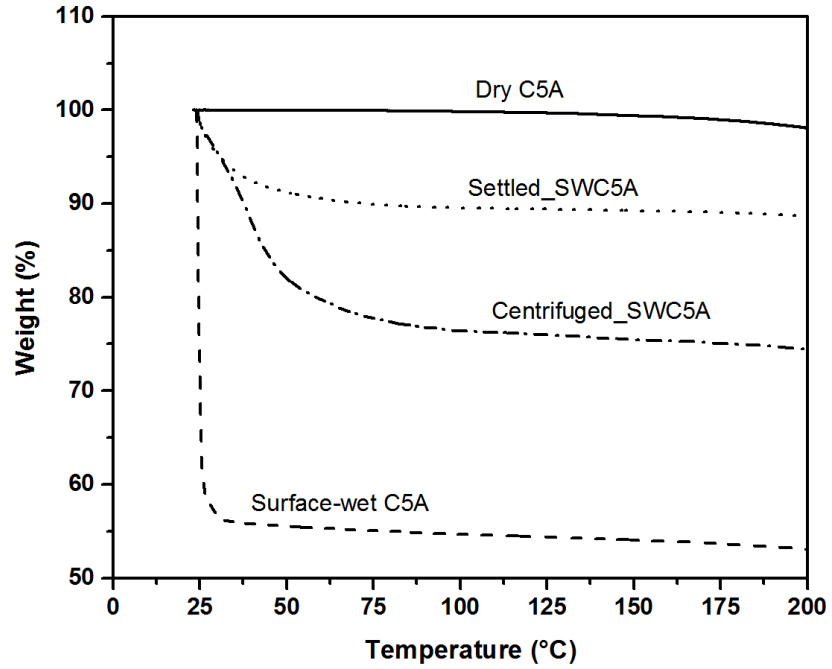


**Figure 4 - 15. Summary TGA profiles of dry C5A, surface-wet C5A, centrifuged SW C5A and settled SW C5A**

## **5. Thermogravimetric Study of Association of Solvent with Clean Clays**

Another source for solvent loss in Tailings Solvent Recovery Unit (TSRU) tailings is the possible interaction of solvent with clays. Model clays, kaolinite and illite were initially considered since they are the most commonly found clays in oil sands ores and tailings. A similar experimental protocol as previously presented was followed. Free solvent on clays will be compared with potential association or trapping of solvent.

In this chapter, the interaction of C5 solvent (60% *n*-pentane and 40% *i*-pentane) with dry and water wet clays is investigated. Thermogravimetric analysis is once again utilized to analyze sample weight loss as a function of increasing temperature for both dry and water-wet (WW) clays with/without C5 solvent. In comparing the weight loss of solvent-wet (SW) clay to dry clay, the amount of solvent interaction with the clay sample can be determined.

### **5.1 Free Solvent in Clean Clays**

#### **5.1.1 Kaolinite**

Kaolinite is the most spherical mineral with the lowest aspect ratio [59]. The chemical formula of kaolinite is  $\text{Al}_4\text{Si}_4\text{O}_{10}(\text{OH})_8$ . Kaolinite is a 1:1 type layered silicate mineral, with one tetrahedral sheet linked through oxygen atoms to the alumina octahedral layer [60]. The structure of kaolinite is shown in Figure 5 – 1.

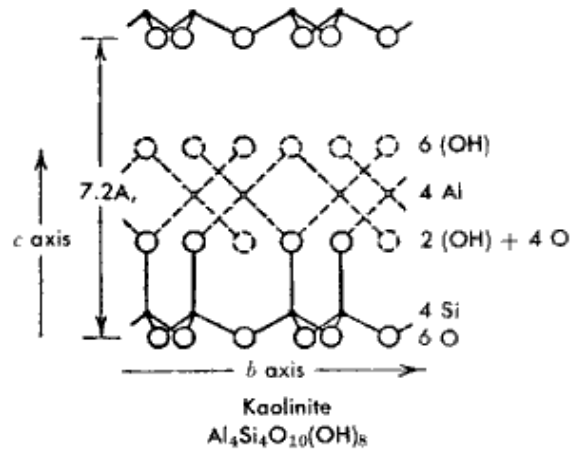


**Figure 5 – 1. Structure of kaolinite [60]**

An FTIR spectra for dry kaolinite is shown in Figure 5 – 2, providing a fingerprint of the kaolinite structure. The peaks at  $900 - 1100 \text{ cm}^{-1}$  and  $3550 - 3750 \text{ cm}^{-1}$  represent stretching of the Si-O bond and the Al-OH deformation in kaolinite. The aromatic C=C stretching is observed by the peak between  $1530 - 1790 \text{ cm}^{-1}$  [22].

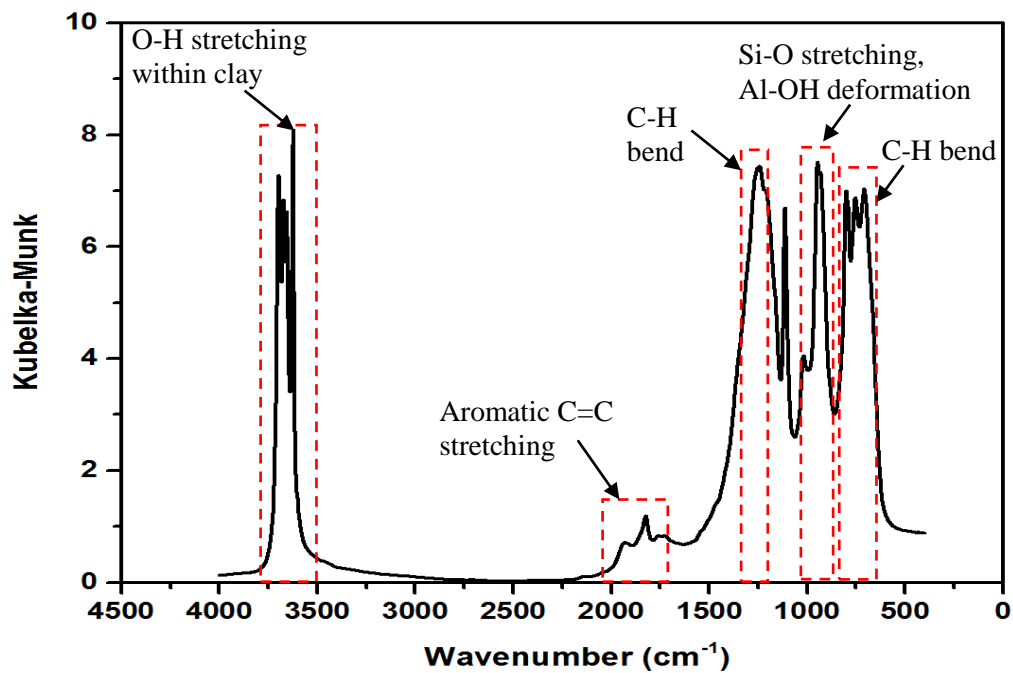


**Figure 5 – 2. FTIR spectra of kaolinite**

To consider removal of free solvent from clay particles, two to three drops of C5 solvent was directly added to both dry and WW kaolinite before immediate analysis using the TGA.

Figure 5 – 3 shows the control TGA profiles for dry and WW kaolinite, and repeats of such experiments with the direct addition of C5 solvent (2-3 drops). Dry kaolinite shows no weight loss up to 400°C. WW kaolinite shows a 20% weight loss by 60°C, due to the removal of water.

With C5 solvent added to dry or WW kaolinite, complete solvent removal is observed at low temperatures (~ 24°C, temperature at which rate of weight loss becomes equivalent to dry case). Such a statement is more conclusive for the dry kaolinite case. Above 24°C all the added C5 solvent to the dry kaolinite sample has been removed. However, the same cannot be said for WW kaolinite at 24°C, because this may include some loss of water weight. A concrete conclusion differentiating between solvent and water loss is difficult to make. Other techniques such as FTIR need to be used. This observation is different when compared to free solvent on asphaltenes (which are surface-wet asphaltenes) that do not lose all the free solvent at 24°C, instead lose the free solvent at 30°C. This is expected because pure kaolinite is very hydrophilic and will most likely not interact with the hydrophobic solvent within a short contact time.

The removal rate of the solvent from the dry and WW kaolinite for a temperature range of 24°C to 25°C is about 7.7%/°C and 10.6%/°C, respectively. These rates

are different because they are dependent on the amount of solvent that was initially added to the clay and the fact that the WW kaolinite rate may be influenced by the removal of water. C5 in general is a very volatile solvent and it is difficult to add a constant volume of C5. Therefore, this may change the removal rate of solvent from the clay. The rate change of the dry kaolinite, free solvent in dry kaolinite, WW kaolinite, and free solvent in WW kaolinite are equivalent at 63°C, which indicates that all added solvent and water has been removed and all systems are completely dry. The removal rate of the water from the WW kaolinite is about 0.73%/°C, which is found from the slope of the TGA profile of the WW kaolinite for a temperature range of 25°C to 63°C. At this same temperature range, the removal rate of water from the system with free solvent in WW kaolinite is about 0.68%/°C, which is within error when compared to the removal rate of water from the pure WW kaolinite system. Therefore, at this temperature range of 25°C to 63°C, only water is being lost from the solvent. Any free solvent present in the system was lost immediately at 24°C.

The weight loss of WW kaolinite is compared to the weight loss of pure water with increasing temperature. Figure 5 – 4 shows the typical shape of water removal compared to the WW kaolinite weight loss curve, showing a strong resemblance of water removal up to ~ 65°C. The temperature at which all water is removed from WW kaolinite is dependent on the volume of water present. The removal rate of water from kaolinite is 0.73%/ °C, which is within error when compared to the removal rate of water of 0.75%/°C for a temperature range of 25



°C to 63 °C. These similar rates signify that only water is being lost from the WW kaolinite. These rates are calculated for the same temperature range by calculating the slopes of the TGA profiles. The loss of water at a temperature lower than its boiling point is due to the flow of purge gas, nitrogen, over the sample in the TGA furnace.

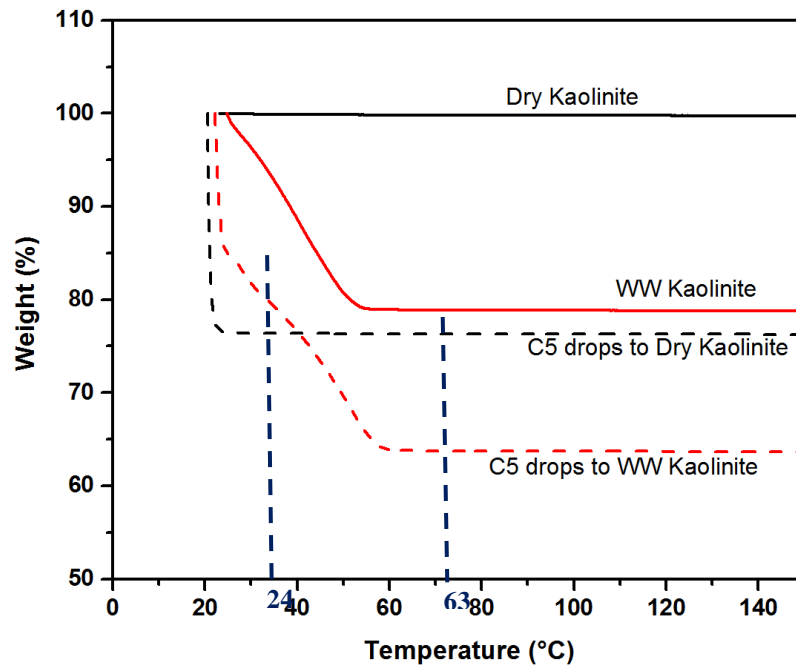


**Figure 5 – 3. Effect of “free” solvent on dry and WW kaolinite**

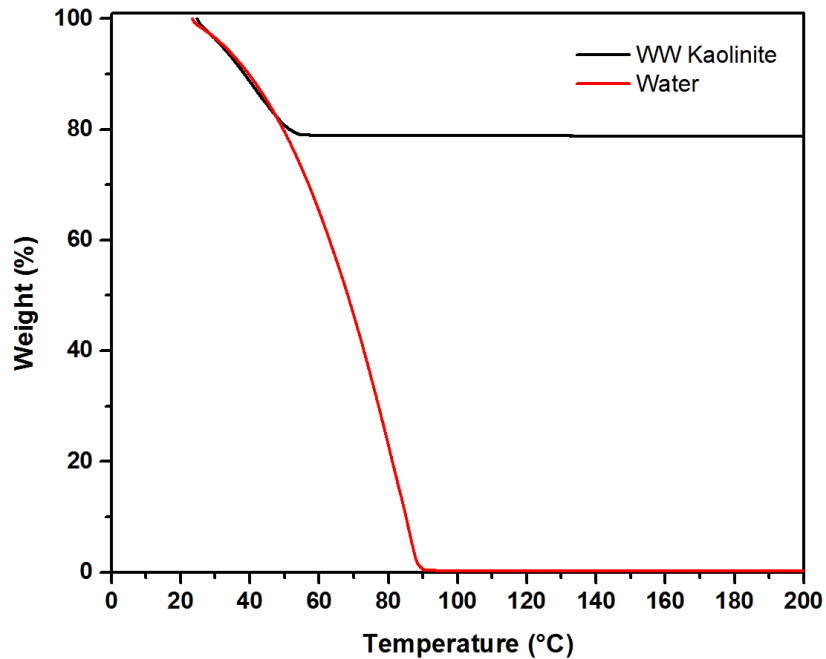


**Figure 5 – 4. TGA profile of WW kaolinite and water with the temperature ramp of 5°C/min up to 150°C, then 10°C/min up to 200°C.**

### 5.1.2 Illite

Illite is a 2:1 three-structured layer consisting of a repetition of a tetrahedron-octahedron-tetrahedron layer [61]. A model of the structure is shown in Figure 5 – 5.

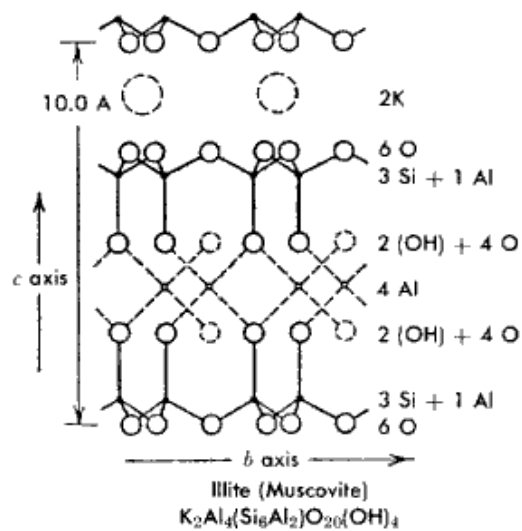


**Figure 5 – 5. Structure of illite [61]**

An FTIR spectrum of dry illite is shown in Figure 5 – 6. The peak at  $3600\text{ cm}^{-1}$  represents the O-H stretching in illite and the peak between  $1600\text{ cm}^{-1}$  and  $1900\text{ cm}^{-1}$  represents the stretching of aromatic C=C. Other peaks observed are due to the bending of C-H [22].

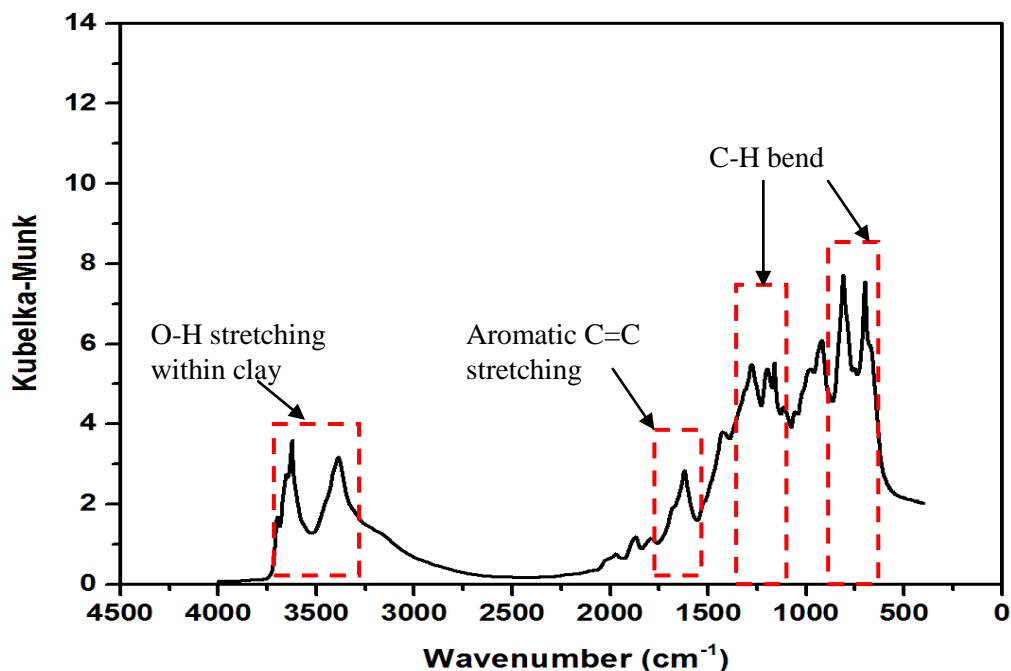


**Figure 5 – 6. FTIR spectra of illite**

The illite was then studied with the TGA to understand its interaction with free solvent. Figure 5 – 7 shows the dry and WW illite TGA response compared to those when free C5 solvent (60% *n*-pentane and 40% *i*-pentane) were added to them. Dry illite loses about 2.5% weight at 100°C, different than what was observed with dry kaolinite (only 0.25% weight loss at 100°C). The weight loss of illite before 100°C is due to water desorption from illite [62]. As observed with kaolinite, when C5 solvent drops are added to dry illite, the solvent is removed quickly, confirming that the free solvent does not associate in any way with the illite. Illite is hydrophilic as well and shows a strong affinity for water, similar to kaolinite [61]. Therefore, the intermolecular forces are weak and there is no attraction of the illite and the hydrophobic aliphatic chain that makes up the solvent. The temperature at which the rate changes of free solvent in dry illite as

compared with the dry illite are equivalent is at 24°C. At this temperature, the free solvent has also been lost from the WW illite, showing that the water film around the clay particle does not interact with solvent. The removal rate of the solvent from the dry illite and WW illite is about 6.4%/°C and 6.9%/°C, slightly lower than solvent removal from kaolinite. However, this rate is dependent on the amount of solvent initially added to the system.

In comparing the drying rates of dry and WW illite and free solvent in dry and WW illite, equivalent conditions are met at 62°C. At this temperature, all added solvent and water is completely removed and all systems are dry. This temperature is similar to the critical temperature found with the kaolinite system.

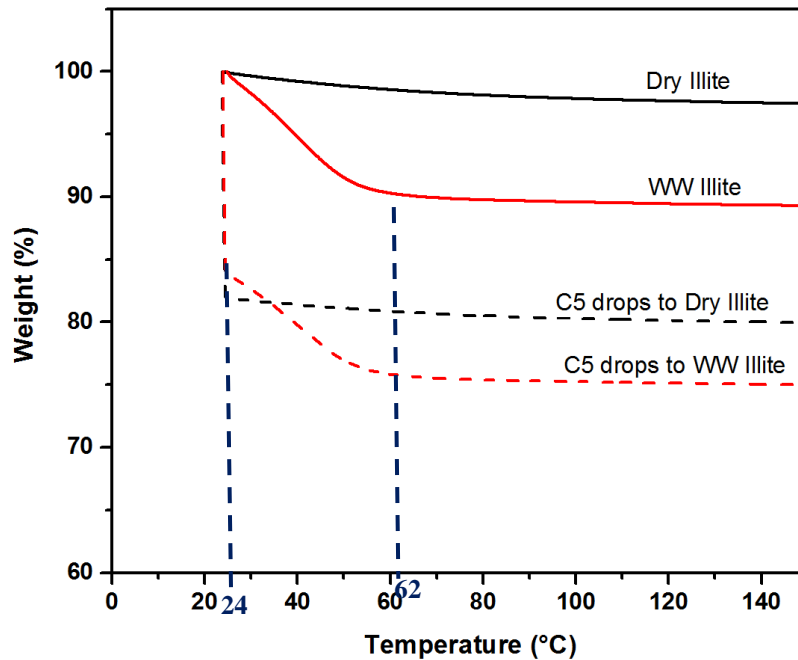


**Figure 5 – 7. Effect of free solvent on dry and WW illite**

## **5.2 Association of Paraffinic Solvent with Clays**

A typical TSRU operates around 75-95°C. Even though this temperature is higher than the boiling point of C5 solvent, the solvent is not completely evaporated and collected from the TSRU tailings. This leads us to believe that there is an interaction of solvent with clays, asphaltenes, or both.

To investigate the interaction of solvent with clean clays, kaolinite and illite were used. C5 solvent (60% *n*-pentane and 40% *i*-pentane) was mixed with clay for 24 hrs to provide sufficient time for solvent interaction with clays. The amount of weight loss in the range of 90-100°C of solvent-wet clays is compared with the weight loss of dry clays at the same temperature range. If there is a difference, this would show the presence of solvent at higher temperatures than its boiling point, hence proving association between the solvent and clays. If there is no difference and the weight loss is exactly the same, then this shows that the solvent is not associated or trapped in the clays.

### **5.2.1 Dry kaolinite**

The TGA profiles for dry kaolinite mixed with C5 for 24 hrs is compared with the TGA profile for dry kaolinite as shown in Figure 5 – 8. The TGA signal was zoomed in the range of 25-150°C to show the small amount of difference in weight loss (~1%). Such behavior suggests that clean, dry kaolinite traps a very small amount of C5 solvent. This means hydrophilic kaolinite molecules cannot bond strongly with the hydrophobic aliphatic chain. The neutral siloxane surfaces found on kaolinite are hydrophobic, so this results in a slightly higher affinity to

hydrocarbon chains such as non-polar solvents. This interaction has been previously reported as well [63]. However, there isn't much literature present on the exact mechanism for the interaction of solvent with kaolinite.

Mikula et al. [47] also found this phenomenon by showing that 1% solvent is trapped within the kaolinite structure. At a critical temperature of 108°C, the rate change of the solvent-wet kaolinite is equivalent to the rate change of the dry kaolinite. This means that at this temperature, all the “associated” solvent has been removed from the clay and it now represents a dry system.

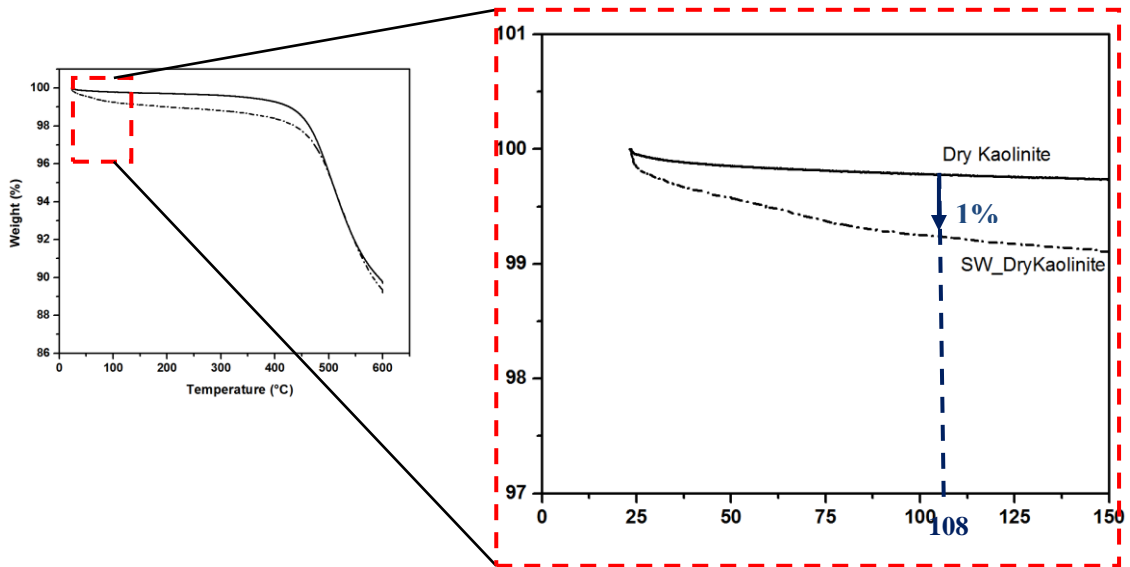


**Figure 5 – 8. Weight loss as a function of temperature when dry kaolinite is mixed with C5 solvent for 24 hrs**

### 5.2.2 Dry illite

The TGA signal of dry illite mixed with solvent and compared with the dry illite TGA signal shows a small difference in weight change as seen in Figure 5 – 9. Therefore, focusing in the range of 25-150°C shows a difference in weight loss of ~ 0.5 wt% from the solvent-wet illite to the dry illite (2.5 wt% loss of dry illite compared to 3 wt% loss of SW illite at the same temperature). This is a little lower than the trapping of solvent in kaolinite. This has been proved before where the illite has a lower affinity for the non-polar solvents in comparison to kaolinite [63]. At a critical temperature of 106°C, the rate change of the solvent-wet illite is equivalent to the rate change of the dry illite signifying that at this temperature the solvent is completely removed from the SW illite. Although not significant, dry illite does play a minor role in the trapping of solvent.

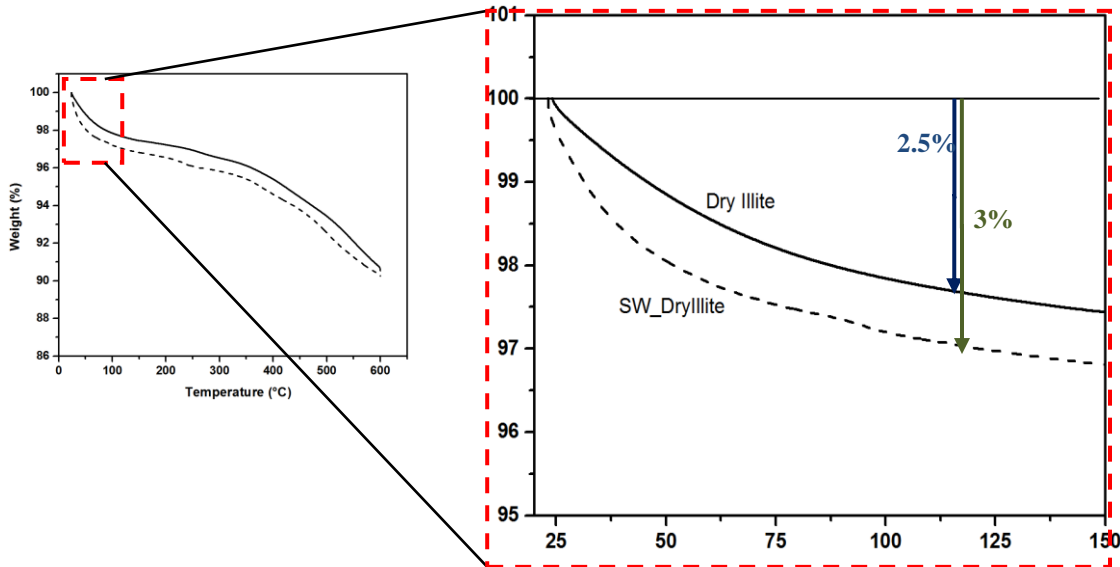


**Figure 5 – 9. Effect of increasing temperature on the weight loss of dry illite when mixed with C5 solvent for 24 hrs**



### 5.2.3 Water-wet kaolinite

The presence of water in kaolinite may impact its interaction with C5 solvent. To test this hypothesis, WW kaolinite was mixed with C5 solvent for 24 hrs and then analyzed with the TGA. The results from this experiment are shown in Figure 5 – 10. These profiles are compared with the WW kaolinite profile. The total weight loss of the SW-WW kaolinite at 108°C is about 12 wt%. At this temperature, the rate change of the SW-WW kaolinite is equivalent to that of the dry kaolinite, signifying that all the water and solvent has been lost and it represents a dry system. Comparing these TGA profiles with the water profile, it is seen that the slope of the mixture (WW kaolinite and solvent) is the same as the slope of the WW kaolinite profile. This means that if there was any solvent interaction with the WW kaolinite, then this was present at the surface and the free solvent may have evaporated even before the TGA measurement started. The water film around the clay particle acted as a barrier and prevented the interaction of solvent with the clay. However, it is difficult to completely differentiate between the water loss and solvent loss from the sample. Therefore, it is highly recommended that other techniques such as FTIR and/or GC-MS be used to study the off-gas from the sample to get a better understanding of the solvent interaction with water-wet clays.

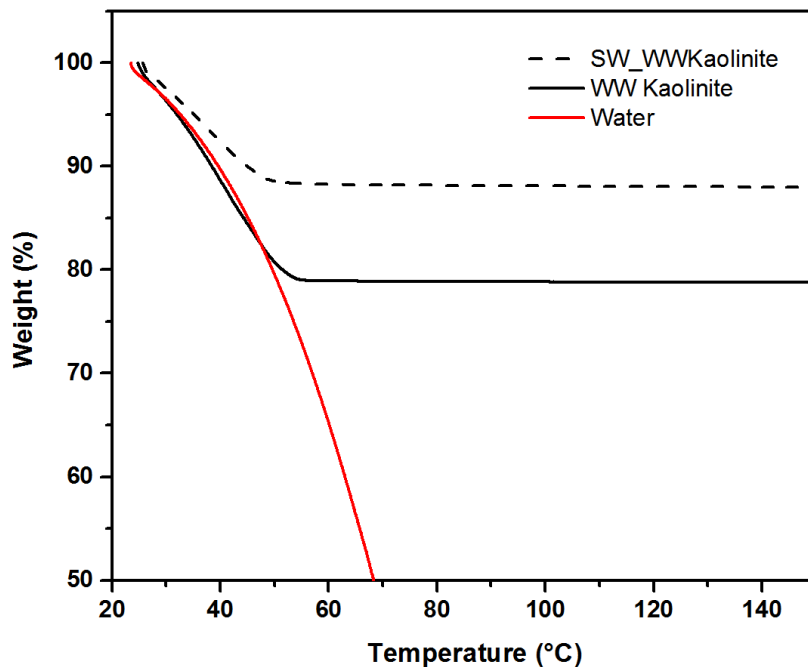


**Figure 5 – 10. Weight loss vs. temperature of WW kaolinite when mixed with C5 solvent for 24 hrs**

#### **5.2.4 Water-wet illite**

The thermogravimetric analysis for the WW illite when mixed with solvent was also carried out and the results are shown in Figure 5 – 11. The total weight loss as a function of temperature of the SW-WW illite is 27% at 100°C. However, this includes the weight loss of water as well. When the WW illite profile is compared with the SW-WW illite profile, the slopes are exactly the same; therefore, the presence of solvent cannot be detected by just performing a thermogravimetric analysis. However, because the slopes are similar, there is most likely an insignificant amount of trapped solvent. Again, it is important to reinforce the

need to use other techniques to study the off-gas from the sample to completely understand solvent interaction with wet clays.

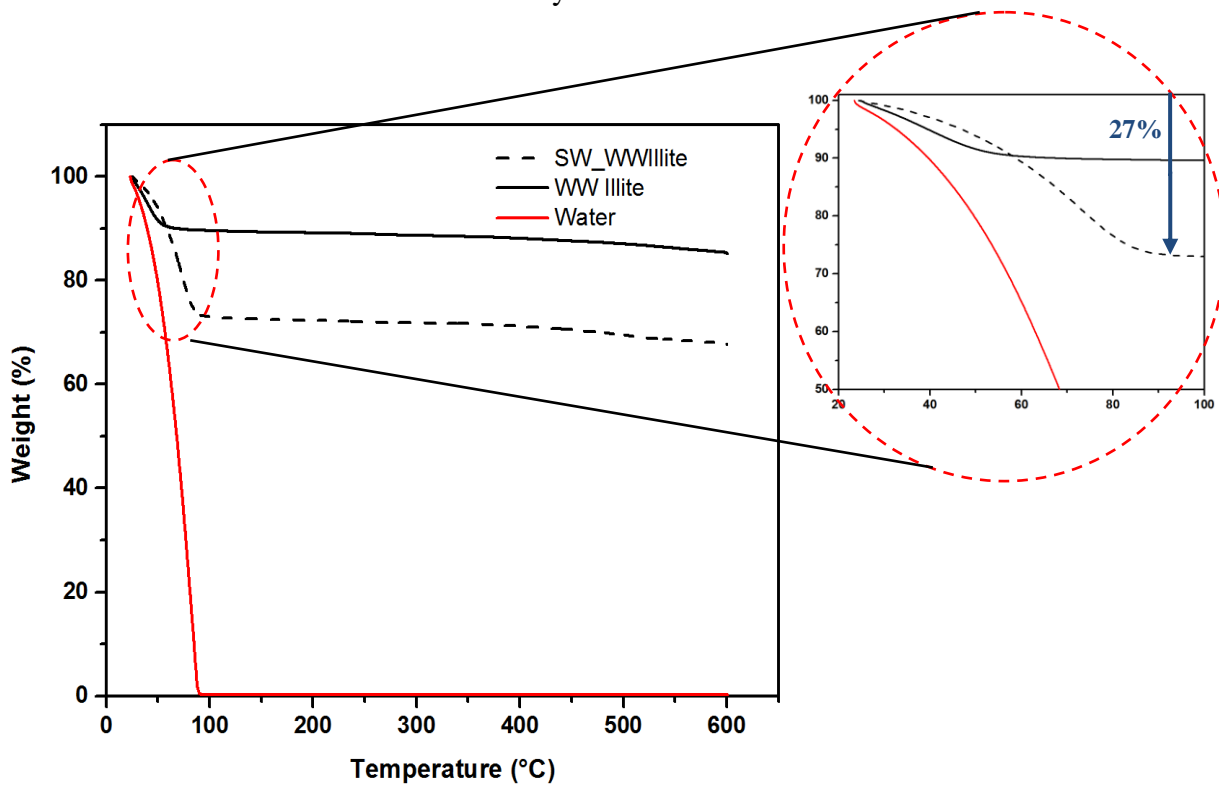


**Figure 5 – 11. Effect of increasing temperature on weight loss of WW illite when mixed with C5 solvent for 24 hrs**

Figure 5 – 11 compares the WW illite with just water and it is interesting to note that the plots do not superimpose like the WW kaolinite curve. This is due to the fact that in contrast to the dry kaolinite, dry illite loses about 2.5% weight at 100°C. Therefore, the WW illite TGA profile does not only show the loss of water at 100°C, but also the loss of dry illite due to a structural change.

### 5.3 Chapter Conclusions

In summary, we found that dry kaolinite trapped about 1 wt% C5 solvent while dry illite trapped a lower amount of 0.5 wt%. When C5 drops were added to both clays, no solvent interaction in clays is observed. Water from the WW kaolinite system and WW illite system is removed at a temperature of 63°C and 62°C respectively. However, the associated solvent from the solvent-wet kaolinite and solvent-wet illite is removed at a temperature of 108°C and 106°C, which means that even if the TSRU is operating at 90°C, this is not sufficient to completely remove the solvent. Although it was shown that water-wet clays do not trap significant amounts of solvent, other techniques such as FTIR or GC-MS need to be used to completely differentiate between water and solvent loss. The composition of the clays in the TSRU tailings is around 10% or even higher. Therefore, although clays do not trap as much solvent as the asphaltenes do, this small 1% may be significant depending on the amount of clays present in TSRU tails.

## **6. Mixed Systems of Asphaltenes, Clays, Water and C5 Solvent**

In reality, tailings consist of mostly water and clays, along with asphaltenes and unrecovered hydrocarbon solvent. It is possible that solvent that is lost with tailings may be trapped in a mixture of asphaltenes and clays and therefore is not recovered in the Tailings Solvent Recovery Unit (TSRU).

In previous chapters, asphaltenes and dry/WW clays were studied independently with the hydrocarbon solvent to understand if there is any association or trapping of solvent. In this chapter, a mixed system with asphaltenes and clays are studied. On a basis of comparison with and without clay, the amount of solvent trapped is measured. Furthermore, investigation of MFT solids and their interaction with C5 solvent (60% *n*-pentane and 40% *i*-pentane) also studied.

### **6.1 Water in Solbit System**

To begin to mimic model froth, water was added to the solbit mixture at a ratio of 1:1.7:0.5 B/S/W and mixed for 24 hrs. An emulsion is formed during mixing because water and solbit are immiscible. Figure 6 – 1 shows the results of asphaltenes that are precipitated in the presence of water; hence labeled as WW-SWC5A. This may include both free asphaltenes and water-oil interfacial asphaltenes. There is a large weight loss up to approximately 100°C, with the weight loss profile comparing with water. If the WW-SWC5A had no association with C5 solvent, and only water present, then the curve would match well with the

water profile. However, when zoomed in at a temperature range of 25-200°C, it can be clearly seen that the profiles do not match and the slopes are different. It can be hypothesized that the slower rate of weight change of the WW-SWC5A is due to the asphaltenes at the interface of a water droplet, which is in turn hindering removal. Asphaltenes stabilize the water droplet, which is hard to remove, compared with only free water which can easily evaporate. Hence, a slightly higher temperature is required to remove mostly water from the WW-SWC5A system. Also, the total weight loss of the WW-SWC5A is much greater than the total weight loss of SW C5A at a specific temperature due to the presence of water. Since it is difficult to determine the degree of solvent interaction, other techniques must be used to differentiate solvent loss from water loss.

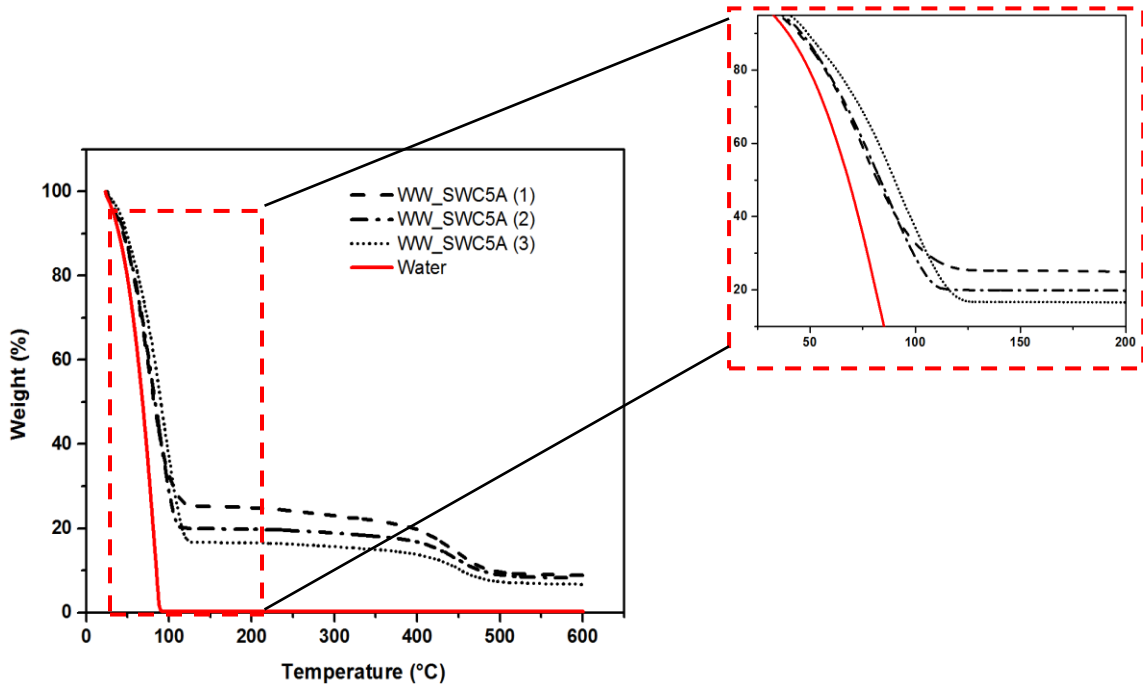


**Figure 6 – 1. TGA profile of three tests of WW-SWC5A compared to TGA profile of only water**

## **6.2 Clays in Solbit System**

The addition of clays to solbit was also investigated to understand if the presence of clays with asphaltenes changes the solvent interaction potential. Four different clays were analyzed: dry kaolinite, dry illite, WW kaolinite, and WW illite. For each batch prepared, 5 g of clay was added to 50 mL of solbit solution. The wet cake after washing with excess solvent was then analyzed using TGA.

### **6.2.1 Effect of dry and WW kaolinite in solbit**

Figure 6 – 2 shows the effect of mixing kaolinite in solbit and then centrifuging to collect the asphaltenes. 5g of clay was added to 50mL of solbit. In the presence of dry kaolinite, asphaltenes trap only 6 wt% of solvent at 100°C, which is lower than the total weight loss of SW C5A (24 wt%) and therefore the association with solvent is reduced. This lower mass makes sense because the presence of clay in the system would mean that the volatile mass is reduced. However, in the presence of WW kaolinite, asphaltenes tend to show a greater weight loss, about 21 wt%. This mass loss includes the mass loss due to evaporation of water from the sample. With a mixed system, it is difficult to understand the degree of association of solvent. The solvent loss is most likely dominated by asphaltene phase. However, we need to probe further studies to identify the time and amount of solvent coming off from the sample.

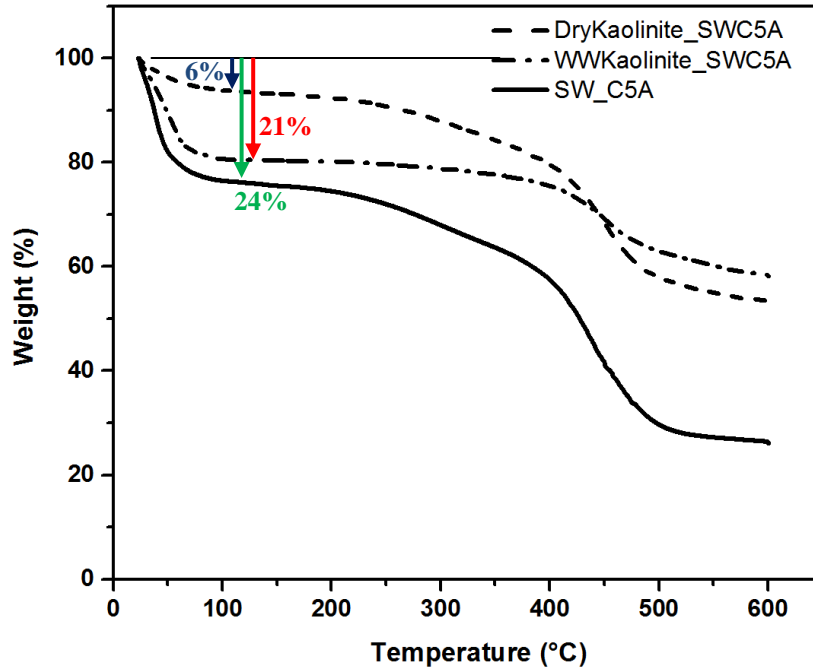


**Figure 6 – 2. Effect of dry/WW kaolinite in SW C5A on the weight loss with increasing temperature**

### 6.2.2 Effect of dry and WW illite in solbit

Similar results are obtained when illite is mixed in solbit and then the C5A are analyzed with the TGA. Figure 6 – 3 shows the effect on the weight loss of the sample in the presence of illite. Dry illite and C5A when mixed together, reduce the amount of solvent apparent weight loss (5 wt% loss) as compared to without dry illite with C5A (24 wt% loss) at 100°C. WW illite when mixed with solbit loses more weight (20 wt%) than solbit mixed with dry illite at 100°C. The greater mass loss is due to the presence of water in the WW illite and the evaporation of water from the sample. Again, it will be stressed here that further studies using FTIR and GC-MS need to be carried out to quantify the amount of



solvent weight loss from these mixed systems and the temperature at which the solvent is completely removed.

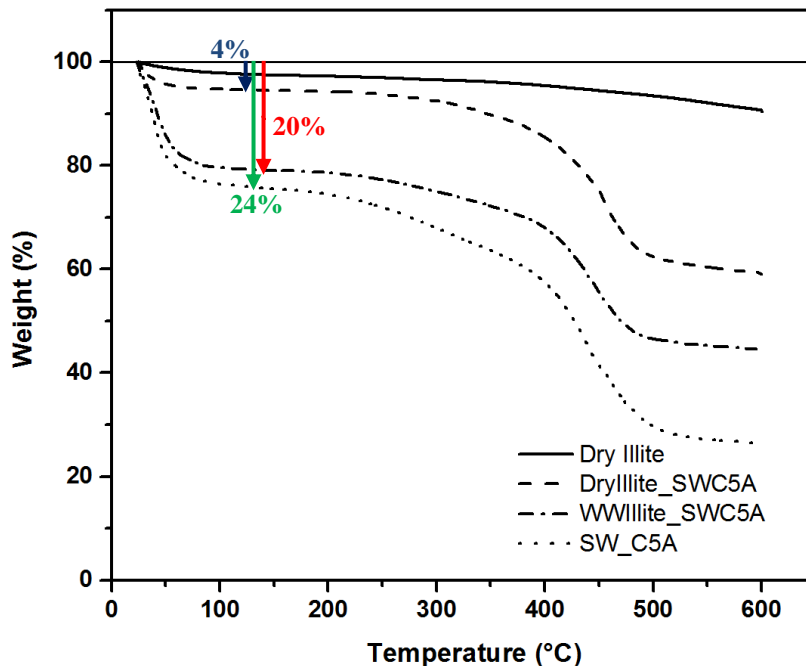


**Figure 6 – 3. Effect of dry/WW illite in SW C5A on the TGA profile**

It has been hypothesized that wettability is related to the nature of the cleavage plane of both clays. With kaolinite, the expected cleavage will lead to an Al-OH plane and a Si-O plane, where the cleavage of illite leads to two Si-O planes. Therefore, the illite would have less exposed Al-OH functional groups (polar groups) on its surface [64]. Bantignies et al. [64; 65] hypothesized that the interaction of asphaltenes with the solid clay surface may be related to the interaction with surface Al-OH and Si-O functional groups. Using FTIR and X-ray adsorption spectroscopy (XAS), Bantignies et al. [65] showed that only Al-OH functional groups interact with the asphaltene polar groups. The local

environment of Al in kaolinite changes during adsorption; however, the Si environment remains unaffected as proved by XAS analysis [65]. The polar groups of the clay attract the asphaltene polar groups, hence causing a lower association with the non-polar groups of the solvent. This explains the lower association with solvent in the presence of clays as seen in our study. However, the amount of clay in the asphaltene sample was not quantified and this may affect the potential interaction with solvent.

### **6.3 MFT**

The MFT solids analyzed to develop an understanding on solvent interaction with organic matter contaminated clays. MFT was diluted with toluene to form three layers: coarse dark layer, fines light layer and fines dark layer so that the toluene insoluble fractions, such as humic matter could be studied. The three layers were separated and each layer was dried in a vacuum oven overnight at 100°C to obtain the solids. The solids collected from the three layers were mixed with C5 solvent for 24 hours to see if there was any interaction with these solids by analyzing the solvent-wet solids with the TGA.

The results can be seen in Figure 6 – 4. For each of the three layers, both dry and solvent-wet solids were analyzed with the TGA. The SW light fines and SW dark fines lose exactly the same amount of weight as the dry light fines and the dry dark fines at each temperature. The light and dark fines solids do not interact with excess solvent. Therefore, the organic matter coated surface prevents solvent interaction. However, with the coarse layer solids, the SW coarse solids showed a

greater weight loss (0.5 wt%) than dry coarse solids. The SW coarse solids are essentially clean solvent interaction with clean minerals. This observation is in agreement with the clay study as explained in Chapter 5.

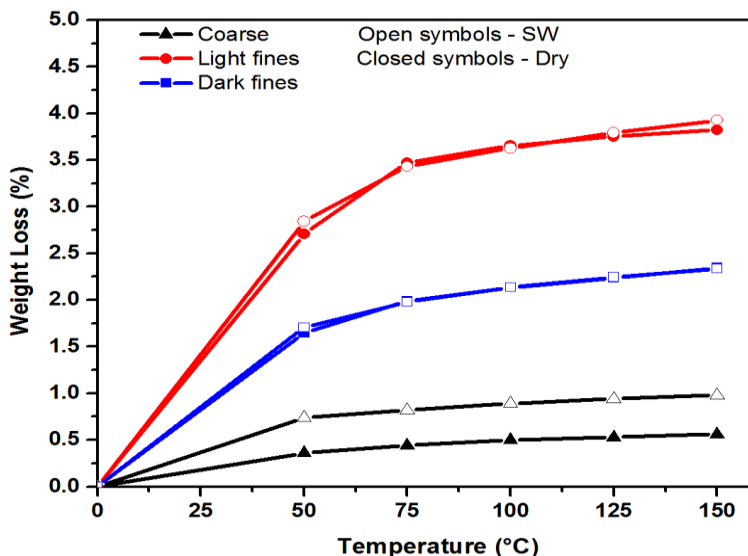


**Figure 6 – 4. Weight loss with increasing temperature when MFT solids are mixed with C5 solvent**

## 6.4 Chapter Conclusions

In summary, this chapter has shown that the presence of clays in asphaltenes hinders the interaction with solvent, resulting in a lower weight loss. Dry kaolinite mixed with SW C5A shows a weight loss of about 6 wt% while dry illite mixed with SW C5A shows a weight loss of about 4 wt% at a temperature of 100°C. This amount of solvent may be different because the amount of clay in the sample was not quantified. However, when there is no presence of clays, SW C5A lose about 24 wt% by 100°C. It is strongly recommended that to quantify the amount of solvent interaction in mixed systems, TGA – FTIR – GC-MS be used.

## 7. Conclusions and Future Work

### 7.1 Conclusions

To comply with ERCB regulations, solvent loss from the Tailings Solvent Recovery Unit (TSRU) should not exceed 4 bbl/1000 bbl of produced bitumen. The TSRU generally operates between 75-90°C, which is higher than the boiling point of the paraffinic solvent. In this work, the association and trapping of paraffinic C5 solvent (60% *n*-pentane, 40% *i*-pentane) with clays (kaolinite and illite) and asphaltenes in tailings was investigated. Thermogravimetry (TGA) was used in this investigation.

In the case of clays, solvent interaction was smaller. Solvent-wet dry kaolinite trapped about 1 wt% of solvent whereas solvent-wet dry illite trapped only 0.5 wt% of solvent. Water-wet (WW) kaolinite and WW illite also trapped about 1 wt% of solvent. For both kaolinite and illite, the solvent was completely removed at a critical temperature of 108°C and 106°C, respectively. Although solvent interaction was low with the wet clays as well, it is important that other techniques such as FTIR or GC-MS be used to completely differentiate between solvent and water weight loss.

Dry asphaltenes (C5A) show no weight loss in the region of 25 – 200°C. Surface-wet asphaltenes show that the free solvent is not completely removed immediately at 25°C. Instead, the solvent is entirely removed from the system at 30°C, after which the surface-wet asphaltenes resemble the dry asphaltenes. Solvent-wet (SW) asphaltenes that have been centrifuged show a weight loss of 24 wt% of the

original mass by 110°C, which indicates the strong interaction with solvent. Asphaltene aggregates trap the solvent inside their structure and hence this solvent is released at temperatures higher than its normal boiling point. However, this solvent is completely removed at a critical temperature of 110°C, after which the SW C5A resemble a dry system. Two factors that may influence the amount of solvent trapped within asphaltenes are:

- (1) Time of secondary stage washing after precipitation: A solvent-wet C5A sample washed in excess solvent trapped 4 wt% more solvent than a solvent-wet C5A sample that was not washed. Also, dry C5A soaked for different amounts of time showed that soaking for longer than 5 min did not change the amount of solvent interaction with the C5A. Therefore, storing the samples and keeping them solvent-wet did not affect the interaction of solvent with the C5A.
- (2) Settling instead of centrifugation: Settling the SW C5A instead of centrifugation showed that 10 wt% solvent was associated with C5A at 110°C. Therefore, centrifugation does not only contribute to association of solvent with asphaltenes, but also to the “trapping” of solvent within asphaltenes.

Mixed systems of clays and asphaltenes showed that in the presence of clays, asphaltenes trap a lower amount of C5 solvent. This observation was true for both kaolinite and illite. MFT solids were mixed with C5 solvent and it was shown that toluene insoluble organic coating does not associate with excess solvent. Small,

almost negligible solvent association is measured for the coarse light layer which is in agreement with the clay study.

In conclusion, asphaltenes play a significant role in the trapping of solvent whereas dry or wet clays (kaolinite and illite) play only a minor role in trapping of solvent. However, the clays may play a more significant role than asphaltenes if the quantity of clays in the TSRU tailings is greater. Therefore, the solvent that is unable to be recovered in the TSRU is lost with the asphaltenes and clays to the tailings.

## **7.2 Future Work**

Solvent interaction in mixed systems of asphaltenes, clays and water need to be studied more in detail. The amount of kaolinite or illite present in the sample must be determined which will then signify the amount of interaction with the solvent. The best way to analyze would be to use TGA coupled with FTIR and GC-MS; this will provide more information about the off-gas coming from the sample at each time and the quantity being released. Both dry and water-wet clays can be analyzed because the FTIR will show the difference between water weight loss and solvent weight loss. This can also lead to carrying out an adsorption study using Quartz Crystal Microbalance with Dissipation Monitoring (QCM-D) and looking at the rates at which the solvent is being adsorbed by the clay and asphaltenes.

A further study can be carried out by using real TSRU tailings sample that contain solvent in them and then analyzing these solids with the FTIR-TGA to quantify the amount of solvent in these solids or asphaltenes.

## 8. References

- [1] Masliyah, J. (2010). *Fundamentals of Oil Sands Extraction*. Edmonton: University of Alberta.
- [2] Peramanu, S., Pruden, B. B., & Rahimi, P. (1999). Molecular Weight and Specific Gravity Distributions for Athabasca and Cold Lake bitumens and their saturates, aromatics, resin, and asphaltene fractions. *Industrial and Chemical Engineering Research*, 38, 3121-3130.
- [3] Yang, X., Hamza, H., & Czarnecki, J. (2004). Investigation of Subfractions of Athabasca Asphaltenes and Their Role in Emulsion Stability. *Energy & Fuels*, 18, 770-777.
- [4] (2009). *ERCB ST98-2009: Alberta's Energy Reserves 2008 and Supply/Demand Outlook / Overview*. Calgary: Energy Resources Conservation Board.
- [5] Masliyah, J., Zhou, Z., & Xu, Z. (2004). Understanding water-based bitumen extraction from Athabasca oil sands. *The Canadian Journal of Chemical Engineering*, 82(4), 628-654.
- [6] Madge, D. N., & Garner, W. N. (2007). Theory of asphaltene precipitation in a hydrocarbon cyclone. *Minerals Engineering*, 20, 387-394.
- [7] (1978). Oil Sands. In G. L. Baughman, *Synthetic Fuels Data Handbook* (pp. 259-321). Denver: Cameron Engineers, Inc.
- [8] Camp, F. W. (1976). *The Tar Sands of Alberta, Canada*. Denver: Cameron Engineers, Inc.
- [9] Gu, G., Xu, Z., Nandakumar, K., & Masliyah, J. H. (2002). Influence of water-soluble and water-insoluble natural surface active components on the stability of water-in-toluene-diluted bitumen emulsion. *Fuel*, 81, 1859-1869.
- [10] Long, Y., Dabros, T., & Hamza, H. (2004). Analysis of Solvent-Diluted Bitumen from Oil Sands Froth Treatment Using NIR Spectroscopy. *The Canadian Journal of Chemical Engineering*, 82(4), 776-781.
- [11] Romanova, U. G., Yarranton, H., & Schramm, L. L. (2004). Investigation of Oil Sands Froth Treatment. *The Canadian Journal of Chemical Engineering*, 82(4), 710-721.



- [12] Masliyah, J., Zhou, Z., Xu, Z., Czarnecki, J., & Hamza, H. (2004). Understanding Water-Based Bitumen Extraction from Athabasca Oil Sands. *The Canadian Journal of Chemical Engineering*, 82, 628-654.
- [13] Long, Y., Dabros, T., & Hamza, H. (2007). Selective Solvent Deasphalting for Heavy Oil Emulsion Treatment. In O. C. Mullins, E. Y. Sheu, A. Hammami, & A. G. Marshall, *Asphaltenes, Heavy Oils, and Petroleomics* (pp. 511-547). Springer.
- [14] Yang, X., & Czarnecki, J. (2002). The Effect of naphtha to bitumen ratio on properties of water in diluted bitumen emulsions. *Colloids and Surfaces A: Physicochemical and Engineering Aspects*, 211, 213-222.
- [15] Long, Y., Dabros, T., & Hamza, H. (2002). Stability and Settling Characteristics of Solvent-Diluted Bitumen Emulsions. *Fuel*, 81(15), 1945-1952.
- [16] Xu, Y., Dabros, T., Hamza, H., & Shefantook, W. (1999). Destabilization of water in bitumen emulsion by washing with water. *Petroleum Science and Technology*, 17(9), 1051-1070.
- [17] Wu, J., & Dabros, T. (2011). Process for Solvent Extraction of Bitumen from Oil Sand. *Energy & Fuels*.
- [18] Kan, J. (2010). *Patent No. 0282642 A1*. United States of America.
- [19] Nalwaya, V., Tantayakom, V., Piumsomboon, P., & Fogler, S. (1999). Studies on Asphaltenes through Analysis of Polar Fractions. *Industrial & Engineering Chemistry Research*, 38, 964-972.
- [20] Kaminski, T. J., Fogler, S., Wolf, N., Wattana, P., & Mairal, A. (2000). Classification of Asphaltenes via Fractionation and the Effect of Heteroatom Content on Dissolution Kinetics. *Energy & Fuels*, 25-30.
- [21] Groenzin, H., & Mullins, O. C. (2000). Molecular Size and Structure of Asphaltenes from Various Sources. *Energy & Fuels*, 14, 677-684.
- [22] Friesen, W. I., Michaelian, K. H., Long, Y., & Dabros, T. (2005). Effect of Solvent-to-Bitumen Ratio on the Pyrolysis Properties of Precipitated Athabasca Asphaltenes. *Energy & Fuels*, 19, 1109-1115.
- [23] Yarranton, H. W., & Masliyah, J. H. (1996). Molar Mass Distribution and Solubility Modeling of Asphaltenes. *AIChE Journal*, 42 (12), 3533-3543.
- [24] Ostlund, J.-A., Wattana, P., Nyden, M., & Fogler, S. (2004). Characterization of fractionated asphaltenes by UV-vis and NMR self-diffusion spectroscopy. *Journal of Colloid and Interface Science*, 372-380.

- [25] Kotlyar, L. S., Sparks, B. D., Woods, J., Capes, C. E., & Schutte, R. (1995). Biwetted ultrafine solids and structure formation in oil sands fine tailings. *Fue* , 74 (8), 1146-1149.
- [26] Leon, O., Rogel, E., Espidel, J., & Torres, G. (2000). Asphaltenes: Structural Characterization, Self-Association, and Stability Behavior. *Energy & Fuels*, 14, 6-10.
- [27] Mohamed, R. S., & Ramos, A. C. (1999). Aggregation Behavior of Two Asphaltenic Fractions in Aromatic Solvents. *Energy & Fuels*, 323-327.
- [28] Oh, K., Ring, T. A., & Deo, M. D. (2004). Asphaltene Aggregation in Organic Solvents. *Journal of Colloid and Interface Science*, 212-219.
- [29] Long, Y., Dabros, T., & Hamza, H. (2004). Structure of water/solids/asphaltenes aggregates and effect of mixing temperature on settling rate in solvent-diluted bitumen. *Fuel*, 83, 823-832.
- [30] Meadus, F. W., Bassaw, B. P., & Sparks, B. D. (1982). Solvent Extraction of Athabasca Oil-Sand in a Rotating Mill Part 2. Solids—Liquid Separation and Bitumen Quality. *Fuel Processing Technology*, 6(3), 289-300.
- [31] Funk, E. W., May, W. G., & Pirkle, J. C. (1982). *Patent No. 4,347,118*. United States of America.
- [32] Graham, R. J., Helstrom, J. J., & Mehlberg, R. L. (1987). A Solvent Extraction Process for Tar Sand. *Eastern OH Shale Symposium* (pp. 93-99). Lexington: Kentucky Energy Cabinet Laboratory.
- [33] Hooshiar, A., Uhlik, P., Liu, Q., Etsell, T. H., & Ivey, D. G. (2012). Clay minerals in nonaqueous extraction of bitumen from Alberta oil sands Part 1. Nonaqueous extraction procedure. *Fuel Processing Technology*, 94, 80-85.
- [34] Al-Sabawi, M., Seth, D., & de Bruijn, T. (2011). Effect of modifiers in n-pentane on the supercritical extraction of Athabasca bitumen. *Fuel Processing Technol* , 92, 1929-1938.
- [35] Brons, G., & Yu, J. M. (1995). Solvent Deasphalting Effects on Whole Cold Lake Bitumen. *Energy & Fuels*, 9, 641-647.
- [36] Zou, X.-Y., Dukhedine-Lalla, L., Zhang, X., & Shaw, J. M. (2004). Selective Rejection of Inorganic Fine Solids, Heavy Metals, and Sulfur from Heavy Oils/Bitumen Using Alkane Solvents . *Industrial and Engineering Chemistry Research*, 43, 7103-7112.

- [37] Tipman, R., Long, Y., & Shelfantook, W. E. (2001). *Patent No. 6,214,213* . United States of America.
- [38] Kotlyar, L. S., Ripmeester, J. A., & Sparks, B. D. (1990). Isolation and characterization of various types of organic matter in oil sands tailings sludge. *Fuel*, 69(12), 1522-1526.
- [39] Kotlyar, L. S., Ripmeester, J. A., Sparks, B. D., & Montgomery, D. S. (1988). Characterization of oil sands solids closely associated with Athabasca bitumen. *Fuel*, 67(6), 808-814.
- [40] Kotlyar, L. S., Ripmeester, J. A., Sparks, B. D., & Montgomery, D. S. (1988). Characterization of organic-rich solids fractions isolated from Athabasca oil sand using a cold water agitation test. *Fuel*, 67, 221-226.
- [41] Kessick, M. A. (1979). Complex Acids and Their Role in the Stability of Clay Sludges from Oil Sands. *Clays and Clay Minerals*, 27(4), 301-302.
- [42] Kessick, M. A. (1979). Structure and Properties of Oil Sands Clay Tailings. *Journal of Canadian Petroleum Technology*, 18.
- [43] Majid, A., & Sparks, B. D. (1996). Role of hydrophobic solids in the stability of oil sands fine tailings. *Fuel*, 75(7), 879-884.
- [44] Kotlyar, L. S., Morat, C., & Ripmeester, J. A. (1991). Structural analysis of Athabasca maltenes fractions using distortionless enhancement by polarization transfer (DEPT) related <sup>13</sup>C n.m.r sequences. *Fuel*, 70(1), 90-94.
- [45] Sparks, B. D., Kotlyar, L. S., O'Carroll, J. B., & Chung, K. H. (2003). Athabasca Oil sands: Effect of Organic Coated Solids on Bitumen Recovery and Quality . *Journal of Petroleum Science and Engineering*, 39, 417-430.
- [46] Kasperski, K., Munoz, V., & Mikula, R. (2010). Naphtha Evaporation from Oil Sands Tailings Ponds. *Oil Sands Conference* . Edmonton: University of Alberta.
- [47] Afara, M., Munoz, V., & Mikula, R. (2010, December 7). Naphtha Interaction with Bitumen and Clays: A preliminary study. Edmonton.
- [48] Dunn, J. G., & Sharp, J. H. (1993). Thermogravimetry. In *Second Edition: Thermal methods*. John Wiley & Sons Inc.
- [49] Brown, M. E. (2001). *Introduction to Thermal Analysis - Techniques and Applications* (2nd Edition ed.). Secaucus, NJ, USA: Kluwer Academic Publishers.

- [50] Fauth, D. J., Frommell, E. A., Hoffman, J. S., Reasbeck, R. P., & Pennline, H. W. (2005). Eutectic salt promoted lithium zirconate: Novel high temperature sorbent for CO<sub>2</sub> capture. *Fuel Processing Technology*, *86*, 1503-1521.
- [51] Parker, S. S. (1988). *Spectroscopy Source Book*. New York: McGraw-Hill.
- [52] Motta, L. (2007). *Wolfram Research*. Retrieved from <http://scienceworld.wolfram.com/physics/MichelsonInterferometer.html>
- [53] Acevedo, S., Cordero, J. M., Carrier, H., Bouyssiere, B., & Lobinski, R. (2009). Trapping of Paraffin and Other Compounds by Asphaltenes Detected by Laser Desorption Ionization - Time of Flight Mass Spectrometry (LDI - TOF MS): Role of A1 and A2 Asphaltene Fractions in This Trapping. *Energy & Fuels*, *23*, 842-848.
- [54] Acevedo, S., Castro, A., Negrin, J. G., Fernandez, A., Escobar, G., & Piscitelli, V. (2007). Relations between Asphaltene Structures and Their Physical and Chemical Properties: The Rosary - Type Structure. *Energy & Fuels*, *21*, 2165-2175.
- [55] Alvarez, E., Marroquin, G., Trejo, F., Centeno, G., Ancheyta, J., & Diaz, J. A. (2011). Pyrolysis kinetics of atmospheric residue and its SARA fractions. *Fuel*, 3602-3607.
- [56] Liao, Z., Geng, A., Graciaa, A., Creux, P., Chrostowska, A., & Zhang, Y. (2006). Different Adsorption/Occlusion Properties of Asphaltenes Associated with Their Secondary Evolution Processes in Oil Reservoirs. *Energy & Fuels*, *20*, 1131-1136.
- [57] Liao, Z., Zhou, H., Graciaa, A., Chrostowska, A., Creux, P., & Geng, A. (2005). Adsorption/Occlusion Characteristics of Asphaltenes: Some Implication for Asphaltene Structural Features. *Energy & Fuels*, *19*, 180-186.
- [58] Yarranton, H. W., Schoeggl, F. S., George, S., & Taylor, S. D. (2011). Asphaltene-Rich Phase Compositions and Sediment Volumes from Drying Experiments. *Energy & Fuels*, 3624-3633.
- [59] Kaminsky, H. (2008). *Clay Minerals*.
- [60] Deer, W. A., Howie, R. A., & Zussman, J. (1992). *An Introduction to the rock-forming minerals* (2nd Edition ed.). Harlow: Longman.
- [61] Saada, A., Siffert, B., & Papirer, E. (1995). Comparison of the Hydrophilicity/Hydrophobicity of Illites and Kaolinites. *Journal of Colloid and Interface Science*, *174*(1), 185-190.

- [62] Sedmale, G., Cimmers, A., & Sedmalis, U. (2009). Characteristics of illite clay and compositions for porous building ceramics production. *Chemine Technologija*, 18-21.
- [63] Schoonheydt, R. A., & Johnston, C. T. (2006). Surface and Interface Chemistry of Clay Minerals. In F. Bergaya, B. K. Theng, & G. Lagaly, *Handbook of Clay Science* (pp. 87-113). Elsevier Ltd. .
- [64] Bantignies, J. L., Moulin, C., & Dexpert, H. (1997). Wettability contrasts in kaolinite and illite clays: Characterization by infrared and X-ray adsorption spectroscopies. *Clays and Clay Mineral*, 45(2), 184-193.
- [65] Bantignies, J. L., Moulin, C., & Dexpert, H. (1998). Asphaltene adsorption on kaolinite characterized by infrared and X-ray adsorption spectroscopies. *Journal of Petroleum Science & Engineering*, 20(3), 233-237.

## Appendix A: Water droplets added to dry C5A

To test if there is any association or trapping of the water molecule within the asphaltenes, a simple test was carried out. Water droplets were added to dry C5A and the weight loss immediately analyzed with a TGA. Figure A-1 shows the results obtained from this test. This figure shows that the total weight loss of the sample is more than 65% by 90°C. Since dry C5A loses no weight by 90°C, all of the weight loss is attributed to the loss of water from the sample. However, it should also be noted that the temperature at which the water is lost (91°C) will be dependent on the volume of water that is added.

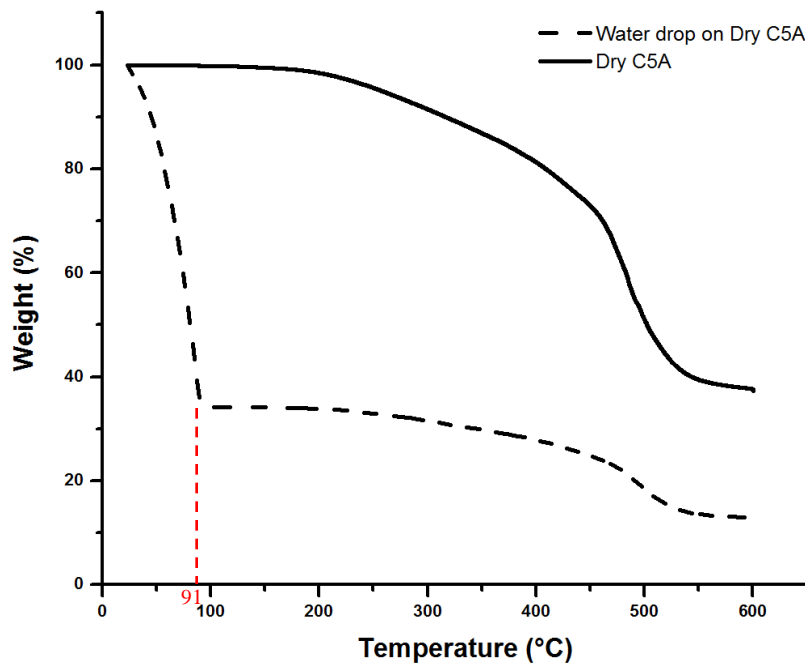


**Figure A-1. TGA profile of water drop added to dry C5A compared to the profile of dry C5A**

Normalized data from Figure A-1 at 100°C is shown in Figure A-2. The normalized mass is calculated starting at 100°C, assuming that the mass of water

has been completely removed. If the water was trapped within the asphaltenes, then weight loss at temperatures higher than 100°C will be observed. It can be seen that the normalized profile overlaps the dry C5A profile, showing that the water droplets have no association with the asphaltene and do not get trapped in the porous structure of the asphaltene.

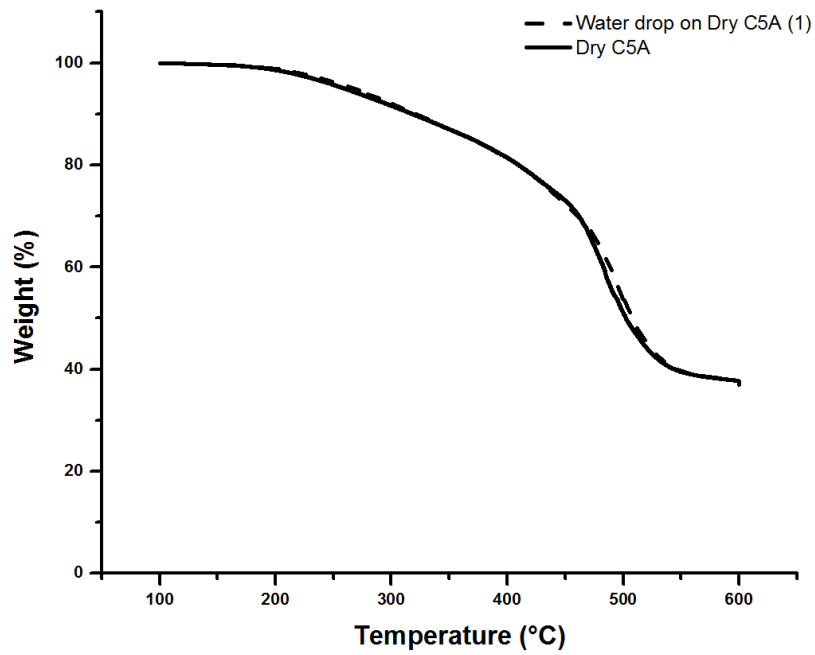


**Figure A-2. Normalized data from Figure A-1 at 100°C to remove water**